Investigations of Platinum Amine Induced Distortions in Single- and Double-Stranded Oligodeoxyribonucleotides

Tammy Page Kline,[†] Luigi G. Marzilli,*[,†,‡] David Live,[†,‡] and Gerald Zon[§]

Contribution from the Department of Chemistry, Emory University, Atlanta, Georgia 30322, and Applied Biosystems, 850 Lincoln Centre Drive, Foster City, California 94404.
Received November 25, 1988

Abstract: The ^{31}P NMR spectrum of *cis*-Pt$(NH_3)_2${d$(T_1C_2T_3C_4G_5G_6T_7C_8T_9C_{10})$-N7(5),N7(6)} has been reported to contain unusual signals with two signals downfield and two upfield of the normal range (ca. −4.0 to −4.4 ppm from trimethyl phosphate standard). This pattern suggested a distorted structure. Since we are interested in metal-induced distortions and only three of the ^{31}P signals have been assigned (G_6pT_7 normal shift, C_4pG_5 upfield, and G_5pG_6 downfield), we have used ^{17}O-labeling methods to identify four additional signals, including the other two unusual signals, as C_2pT_3 and T_3pC_4. $^3J_{H3'-P}$ values were measured by 2D *J* and selective reverse chemical shift correlation spectroscopy. Three ^{31}P signals exhibited unusually large coupling to H3′ (C_2p, 8.9 Hz; T_3p, 8.0 Hz; G_5p, 8.9 Hz). The C4′–C3′–O3′–P torsional angle (ϵ) values, which may reflect averaging of several conformers, correspond to 217° for C_2p and G_5p and 211° for T_3p, compared to ~206° for the normal range signals. Because all these unusual signals are for phosphate groups on the 5′ end of the strand, we evaluated two models for the distortions as follows: (1) model I in which the 5′ region $T_1C_2T_3C_4$ is looped around the Pt moiety, with at least one hydrogen bond with the Pt amine ligands, and (2) model II in which $T_1C_2T_3C_4$ bends away from the Pt moiety and the terminal T_1C_2 bases form base pairs with GG. Further evidence (^1H NMR spectroscopy, electrophoresis, and UV absorbance temperature-dependence studies) was consistent with model I. The lack of ^1H NMR imino signals observed in the 15–11 ppm region indicates that no base pairs are formed. Electrophoretic analysis demonstrates a decrease in mobility of the oligomer upon platination, evidence against a compact structure such as a hairpin. Staining of the electrophoresis band with acridine orange suggested a single-stranded structure. The UV absorbance showed no increase over the range 20–70 °C. The ^{195}Pt NMR signal was observed at −2450 ppm, a value consistent with a normal coordination environment. Limited spectral studies performed on the analogous Pt(en) (en = ethylenediamine) and *cis*-Pt$(MeNH_2)_2$ adducts gave further evidence for model I. The chemical shift of the C_2pT_3 signal and the temperature dependence of one of the upfield signals were sensitive to the nature of the amine ligand. The chemical shift of the downfield GpG ^{31}P signal can be correlated with the potential hydrogen-bonding ability of the amine ligand. The ^{31}P NMR spectrum of the duplex [*cis*-Pt$(NH_3)_2${d(TCTCGGTCTC)-N7(5),N7(6)}]–d(GAGACCGAGA) has two unusual ^{31}P signals previously assigned as G_5pG_6 (−3.2 ppm) and C_4pG_5 (−4.9 ppm). The similarity in values of $^3J_{HCOP}$ for G_5p and C_4p to those measured in the single strand indicates that the backbone structure of the platinated $C_4G_5G_6$ does not change significantly upon duplex formation. Two sequential temperature-dependent structural transitions were evident for solutions of the duplex. The first transition (melting of the duplex) was characterized by sigmoidal changes in chemical shifts of the unusual ^{31}P signals and in UV absorbance and by broadening of the G_5 H8 signal. Formation of the single strand was indicated by the appearance of the downfield C_2pT_3 ^{31}P signal. The second transition (melting of the model I structure) was characterized by a featureless UV absorbance increase, shifting of the C_2pT_3 ^{31}P signal into the normal range, and the appearance of a sharpened G_6 H8 signal.

DNA is probably the primary molecular target of the widely used anticancer drug *cis*-Pt$(NH_3)_2Cl_2$.[1-3] Chromatographic analyses of enzyme digests of DNA treated with anticancer active Pt compounds suggest that -GpG- sites are favored for Pt binding.[4,5] ^{31}P NMR studies of DNA treated with *cis*-PtA_2Cl_2 have demonstrated the appearance of a signal downfield of the normal DNA ^{31}P signal range.[6,7] In a ^{31}P NMR survey of a variety of oligonucleotides treated with *cis*-PtA_2Cl_2,[8] it was found that the spectra of oligonucleotides containing a GpG site each exhibited at least one ^{31}P signal ca. 1.2 ppm downfield of the remainder of the signals at ca. −4.2 ppm. With oligonucleotides not containing a GpG site, no unusually shifted signals were observed in the ^{31}P NMR spectra. Also, the therapeutically inactive *trans*-Pt$(NH_3)_2Cl_2$ compound did not produce any unusual ^{31}P signals upon reaction with DNA or oligonucleotides.

A study of *cis*-PtA_2{d(TGGT)-N7(2),N7(3)}[9] (A_2 = $(NH_3)_2$, en, $(MeNH_2)_2$, tn (tn = trimethylenediamine), Me_2tn, and *N*,*N*-Me_2en)[10] revealed the presence of a downfield ^{31}P NMR signal at ca. −3 ppm.[11,12] HMQC and ^{17}O-labeling studies definitely established that the phosphorus leading to the downfield signal is in the Pt intrastrand GpG cross-link. A correlation was found between the shift of the downfield signal and the potential hydrogen-bonding ability of the Pt amine. Molecular mechanics calculations of [*cis*-Pt$(NH_3)_2${d$(T_1C_2T_3C_4G_5G_6T_7C_8T_9C_{10})$-N7(5),N7(6)}]–d(GAGACCGAGA)[13] and X-ray structures of *cis*-Pt$(NH_3)_2${d(pGpG)-N7(1),N7(2)}[14] and *cis*-Pt$(NH_3)_2${d(CGG)-N7(2),N7(3)}[15] suggest that hydrogen binding between one amine ligand on Pt and the phosphate group 5′ to the GpG

[†] Emory University.
[‡] Member of the Winship Cancer Center.
[§] Applied Biosystems.

(1) Sun, M. *Science (Washington, D.C.)* **1983**, *222*, 145.
(2) Pinto, A. L.; Lippard, S. J. *Biochim. Biophys. Acta* **1985**, *780*, 162.
(3) Reedijk, J.; Fichtinger-Schepman, A. M. J.; van Oosteroom, A. T.; van de Putte, P. *Struct. Bonding* **1987**, *67*, 53.
(4) Fichtinger-Schepman, A. M. J.; Lohman, P. H. M.; Reedijk, J. *Nucleic Acids Res.* **1982**, *10*, 5345.
(5) Fichtinger-Schepman, A. M. J.; van der Veer, J. L.; den Hartog, J. H. J.; Lohman, P. H. M.; Reedijk, J. *Biochemistry* **1985**, *24*, 707.
(6) Marzilli, L. G.; Reily, M. D.; Heyl, B. L.; McMurray, C. T.; Wilson, W. D. *FEBS Lett.* **1984**, *176*, 389.
(7) den Hartog, J. H. J.; Altona, C.; van Boom, J. H.; Reedijk, J. *FEBS Lett.* **1984**, *176*, 393.
(8) Fouts, C. S.; Reily, M. D.; Marzilli, L. G.; Zon, G. *Inorg. Chim. Acta* **1987**, *137*, 1.
(9) Bases in oligonucleotides are numbered starting from the most 5′ base and proceeding in the 3′ direction.
(10) Abbreviations: en = ethylenediamine; $MeNH_2$ = methylamine; DMT = dimethoxytrityl; TEA = triethylamine; TEA A = triethylammonium acetate buffer; HPLC = high performance liquid chromatography; T = thymidine; A = adenine; C = cytidine; G = guanine; EDTA = ethylenediaminetetraacetic acid; TSP = sodium 3-(trimethylsilyl)tetradeuteriopropionate; TMP = trimethylphosphate; PIPES = piperazine-*N*,*N*′-bis(2-ethanesulfonic acid).
(11) Byrd, R. A.; Summers, M. F.; Zon, G.; Fouts, C. S.; Marzilli, L. G. *J. Am. Chem. Soc.* **1986**, *108*, 504.
(12) Fouts, C. S.; Marzilli, L. G.; Byrd, R. A.; Summers, M. F.; Zon, G.; Shinozuka, K. *Inorg. Chem.* **1988**, *27*, 366.
(13) Kozelka, J.; Petsko, G. A.; Quigley, G. J.; Lippard, S. J. *Inorg. Chem.* **1986**, *25*, 1075. A reviewer wished us to emphasize that such molecular mechanics calculations are not a reliable indicator of H bonding since the influence of solvent water molecules was not accurately portrayed.
(14) Sherman, S. E.; Gibson, D.; Wang, A. H.-J.; Lippard, S. J. *Science (Washington, D.C.)* **1985**, *230*, 412.

0002-7863/89/1511-7057$01.50/0

moiety is an important feature of Pt binding.

In recent studies, ^1H and ^{31}P NMR spectroscopy were used to investigate the platinated single-strand *cis*-$Pt(NH_3)_2$[d-$(T_1C_2T_3C_4G_5G_6T_7C_8T_9C_{10})$-N7(5),N7(6)].[7,16,17] The ^{31}P NMR spectrum showed four unusually shifted signals, two downfield and two upfield of the normal range. Based on ^{31}P–^1H decoupling experiments, the most downfield and the most upfield signals were identified as GpG and CpG, respectively. A few ^1H NMR assignments were made, mostly on the basis of 1D NOE results. In the same study, the duplex formed on addition of the complementary strand, $d(G_{11}A_{12}G_{13}A_{14}C_{15}C_{16}G_{17}A_{18}G_{19}A_{20})$, was also investigated. One downfield ^{31}P signal was observed and assigned to G_5pG_6 by ^{31}P–^1H decoupling experiments. The upfield signal, which is unusual,[8] was tentatively assigned to C_4pG_5 on the platinated strand by comparison of chemical shifts at high temperature.[7] Most of the ^1H NMR signals of the duplex, [*cis*-Pt-$(NH_3)_2$[d(TCTCGGTCTC)-N7(5),N7(6)]]–d(GAGACCGAGA), were assigned by 2D methods.[16] ^1H NMR studies of imino and aromatic signals indicated that platination does not disrupt the duplex but rather induces a kink located at the G_5C_{16} base pair.[16,17] Molecular mechanics calculations[13] have suggested that a kinked structure is possible for this duplex. A gel electrophoresis investigation of the *cis*-$Pt(NH_3)_2$ adducts of oligonucleotides containing adjacent G residues demonstrated bending (~40°) at the intrastrand Pt cross-link and toward the major groove, where the Pt is located.[18]

In our examination of the Pt binding to the self-complementary oligonucleotide, $d(TATGGGTACCCATA)_2$,[19] we also found more than one ^{31}P NMR signal shifted out of the normal range. Platination induces formation of single strands which possess an unprecedented type of hairpinlike structure. We wished to investigate well-characterized models for metal-ion-induced oligonucleotide distortions and the application of ^{31}P NMR spectroscopy to the study of the metal binding to DNA. The presence of three unusually shifted ^{31}P NMR signals for *cis*-$Pt(NH_3)_2$[d-(TCTCGGTCTC)-N7(5),N7(6)] and one unusually shifted ^{31}P NMR signal for *cis*-$Pt(NH_3)_2$[d(TCTCGGTCTC)-N7(5),N7-(6)]–d(GAGACCGAGA) in addition to the downfield signal attributable to Pt binding indicated distortion in regions remote from the Pt binding site. Therefore, we investigated the ^{31}P NMR features of these well-characterized systems. We also conducted additional types of experiments, e.g., ^{17}O labeling, ^{195}Pt NMR spectroscopy, paramagnetic probes (such as Cu^{2+}), electrophoresis, and UV spectroscopy. In this manner, we have established criteria with which we can assess the long-range effects of cationic metal species on other oligonucleotides.

Experimental Section

Materials. Oligodeoxyribonucleotides (oligomers) and ^{17}O-labeled oligomers were prepared by the phosphoramidite method.[20-22] The crude DMT-protected material was dissolved in TEA[10] (100 μL), and the volume was reduced to ca. 75 μL with a stream of air to remove excess NH_3. The solution was lyophilized, dissolved in TEA (100 μL):0.1 M TEA A[10] (1600 μL), and passed through a 0.45-μm Millipore filter (syringe). The lyophilization flask was rinsed with TEA A (1.0 mL), and the resulting solution was also passed through the syringe filter. HPLC[10] purification of the resulting DMT-protected oligomer solution was performed on a Hamilton PRP-1 (0.7 × 30.5 cm) column at 60 °C. Eluent A was 0.1 M TEA A and eluent B was HPLC–UV grade CH_3CN. The gradient employed was 20–30% B in 10 min and 30% B for the next 15 min at a flow rate of 3 mL/min.

After lyophilization, the collected material was dissolved in 30% acetic acid. The pH of the resulting solution was adjusted to ca. 3. At this pH, the DMT protecting group is removed in ~30 min. After lyophilization, the residue was dissolved in H_2O (1 mL) and the free DMT was extracted with ethyl acetate (1 mL). The ethyl acetate extraction was repeated twice. The sample was lyophilized and dissolved in 1.0 M NaCl (300 μL), and the oligomer was precipitated with chilled ethanol (1 mL). The supernatant was removed and, after it was checked for oligomer content by UV absorbance at 260 nm, discarded. This procedure was repeated with 1.0 M NaCl (600 μL) and ethanol (2 mL). To complete the purification, a solution of the oligomer in H_2O (1.0 mL) was passed through a 2 × 20 cm Sephadex G-10 column (H_2O eluent, 0.5 mL/min). The absorbance of the eluent was monitored at 254 nm, and the resulting peak was collected.

Solution concentrations are calculated in terms of bases. The ϵ_{260}(25 °C) values were determined in the following manner. The average extinction coefficient per base, $^*\epsilon_{260}$ (uncorrected for base stacking), was calculated by taking the sum of ϵ_{260} for the bases and dividing by the number of bases. For A, G, C, and T,[10] ϵ_{260} values used were 15400, 11700, 7500, and 9200 M^{-1} cm^{-1}, respectively.[23] The absorbance at 260 nm of each oligomer was measured at 25 and at 96 °C (the temperature at which bases are unstacked and $^*\epsilon_{260}$ is assumed to be applicable). An ϵ value for 25 °C was then determined by adjusting $^*\epsilon_{260}$ for base stacking: $\epsilon_{260}(25\ °C) = (A_{25}/A_{96})^*\epsilon_{260}$. Concentrations were determined by using the following ϵ_{260}(25 °C): 8800 M^{-1} cm^{-1} for d-(TCTCGGTCTC); 11 600 M^{-1} cm^{-1} for d(GAGACCGAGA); 9100 M^{-1} cm^{-1} for the d(TCTCGGTCTC)–d(GAGACCGAGA) duplex.

Pt Reactions. *cis*-$Pt(NH_3)_2Cl_2$ was purchased from Aldrich. The Pt compounds $Pt(en)Cl_2$ and *cis*-$Pt(MeNH_2)_2Cl_2$ were prepared by the method of Dhara.[24]

The d(TCTCGGTCTC) oligomer was dissolved in deionized H_2O to a concentration of 0.5–1.0 mM. One equivalent per strand of the desired platinum complex was added, and the solid readily dissolved after stirring for ~5 min. The pH was adjusted to 6.3; EDTA[10] (10^{-4} M) and chloroform (~1 mL) were added as antimicrobial agents. The solution was kept in the dark at ambient temperature for 7–10 days. Progress of the reaction was monitored by HPLC and ^1H NMR spectroscopy. The platinated d(TCTCGGTCTC)–d(GAGACCGAGA) duplex was formed by making a concentrated solution of the complementary strand in H_2O, determining its concentration, and adding the appropriate amount to the *cis*-$Pt(NH_3)_2$[d(TCTCGGTCTC)-N7(5),N7(6)] solution. The ratio of *cis*-$Pt(NH_3)_2$[d(TCTCGGTCTC)-N7(5),N7(6)] to d(GAGACCGAGA) was verified by ^{31}P NMR spectroscopy (see below). Values of ϵ_{260}(25 °C) calculated for the oligomers were also used for the platinated oligomers.

Instrumental Methods. One-Dimensional NMR Spectroscopy. (a) ^1H NMR. Spectra were obtained at 361 MHz with a Nicolet 360-NB spectrometer equipped with a variable-temperature unit. Typical conditions for recording of D_2O solution spectra include 2900-Hz sweep width, 30° pulse width, 200 scans, 0.3-Hz line broadening, and 16K data points. For H_2O/D_2O samples, a Nicolet-modified version of the Redfield 2142-pulse sequence[25,26] was employed with typical conditions: 4000 scans, 1.0-Hz line broadening, and 8K or 16K data points. Sample conditions were typically 0.020 M, pH 6.8, 0.5-mL volume, 99.9% D_2O or 90% H_2O:10% D_2O in 5-mm NMR tubes. D_2O was purchased from Aldrich. TSP[10] ($(CH_3)_3SiCD_2CD_2COONa$ from Aldrich) was used as an internal reference.

(b) ^{31}P NMR. Spectra were obtained at 81.01 MHz with an IBM WP-200SY spectrometer equipped with a variable-temperature unit. Typical conditions for recording spectra include 1300-Hz sweep width, 45° pulse width, 10000 scans, 1.0-Hz line broadening, and 4K data points. ^1H NMR samples, contained in 5-mm NMR tubes, were concentrically placed in 10-mm NMR tubes with the same solvent (with a small amount of TMP[10]) surrounding the insert.

(c) ^{195}Pt NMR. Spectra were obtained at 107.23 MHz on a GE GN-500 spectrometer equipped with a 10-mm broad-band probe and a

(15) Admiraal, G.; van der Veer, J.; de Graff, R. A.; den Hartog, J. H. J.; Reedijk, J. *J. Am. Chem. Soc.* **1987**, *109*, 594.
(16) den Hartog, J. H. J.; Altona, C.; van Boom, J. H.; van der Marel, G. A.; Haasnoot, C. A. G.; Reedijk, J. *J. Biomol. Struct. Dyn.* **1985**, *2*, 1137.
(17) den Hartog, J. H. J.; Altona, C.; van Boom, J. H.; van der Marel, G. A.; Haasnoot, C. A. G.; Reedijk, J. *J. Am. Chem. Soc.* **1984**, *106*, 1528.
(18) Rice, J. A.; Crothers, D. M.; Pinto, A. L.; Lippard, S. J. *Proc. Natl. Acad. Sci. U.S.A.* **1988**, *85*, 4158.
(19) (a) Marzilli, L. G.; Fouts, C. S.; Kline, T. P.; Zon, G. In *Platinum and Other Metal Coordination Compounds in Cancer Chemotherapy*; Nicolini, M., Ed.; Martinus Nijhoff Publishing: Boston, 1987; p 67. (b) Marzilli, L. G.; Kline, T. P.; Live, D.; Zon, G. In *Transition Metal-Nucleic Acid Chemistry*; Tullius, T., Ed.; in press. (c) Fouts, C. S. Ph.D. Thesis, Emory University, 1987.
(20) Broido, M. S.; Zon, G.; James, T. L. *Biochem. Biophys. Res. Commun.* **1984**, *119*, 663.
(21) Stec, W. J.; Zon, G.; Egan, W.; Byrd, R. A.; Phillips, L. R.; Gallo, K. A. *J. Org. Chem.* **1985**, *50*, 3908.
(22) Stec, W. J.; Zon, G.; Egan, W.; Stec, B. *J. Am. Chem. Soc.* **1984**, *106*, 6077.
(23) *Handbook of Biochemistry*; Harte, R. A., Ed.; The Chemical Rubber Co.: Cleveland, OH, 1968.
(24) Dhara, S. C. *Ind. J. Chem.* **1970**, *8*, 193.
(25) Redfield, A. G.; Kunz, S. D.; Ralph, E. K. *J. Magn. Reson.* **1975**, *19*, 114.
(26) Redfield, A. G.; Kunz, S. D. In *NMR and Biochemistry*; Opella, S. J., Lu, P., Eds.; Marcel Dekker: New York, 1979; p 225.

12-bit ADC. Typical conditions for recording spectra include 142857-Hz sweep width, 45° pulse width, 50-Hz line broadening, 1024 data points, and 3.58-ms acquisition time. Five acquisitions of 1 048 565 scans each in double-precision mode were obtained and then block averaged. Sample conditions were 0.003 M Pt, pH 7.0, 0.5 mL, 99.9% D_2O in a 5-mm NMR tube. A 0.1 M solution of Na_2PtCl_6 was used as the reference.

Two-Dimensional NMR Spectroscopy. The following experiments were performed with the GE GN-500 instrument equipped for reverse detection experiments:

(a) Selective Reverse Chemical Shift Correlation (SRCSC). The pulse sequence for this experiment was saturation(^{1}H)–90(^{31}P)–t_1/2–180$_{sel}$(^{1}H)–180(^{1}H)–t_1/2–90(^{31}P)–90(^{1}H)–acquire(^{1}H)[27,28] (t_1 is the evolution time in the ^{31}P dimension). The sweep width in the ^{1}H dimension was 1300 Hz in 1024 points for an acquisition time of 787 ms. Collected were 128 blocks of 64 scans each. The power of the selective pulse was 125 Hz in units of γH_2, with the transmitter set at 4.8 ppm. Alternate scans were stored in separate areas of memory and processed to yield a phased 2D spectrum.[27,28] The sweep width in the ^{31}P dimension was 600 Hz with an effective acquisition time in that dimension of 107 ms. The ^{31}P dimension was zero-filled twice before processing, and the resulting phased 2D spectrum showing both positive and negative contours is shown. This experiment selects for H3′-P correlations, and the splitting of the signal in the ^{31}P dimension is the result of vicinal coupling between these nuclei.

(b) Heteronuclear 2D *J*. The pulse sequence used was 90(^{1}H)–t_1/2–90$_{sel}$(^{1}H)–180(^{31}P)–90$_{sel}$(^{1}H)–t_1/2–acquire(^{1}H)decouple(^{31}P).[28] The ^{1}H sweep width was 1300 Hz with a size of 1024 points for an acquisition time of 787 ms. Collected were 64 blocks of 64 scans each. The magnitude of the selective pulse was 119 Hz in units of γH_2 centered at 4.75 ppm. The spectral width in the f_1 dimension was 50 Hz with an effective acquisition time of 1.28 s. The f_1 dimension was zero-filled twice before processing. Data are presented in phase-sensitive mode.

(c) NOESY. The pulse sequence used was 90°–t_1–90°–τ_m–90°–acquire.[29] A mixing time of 700 ms and a sweep width of 5000 Hz in both dimensions were used. Collected were 512 blocks of 32 scans and 1024 data points each at 32 °C. The structure is conformationally mobile, and long mixing times were required to obtain the relatively few cross peaks observed.

HPLC. HPLC purifications and analyses were performed on Rainin Rabbit Gradient HPLC systems with either a Hitachi 100-30 spectrophotometer set at 260 nm or a LDC/Milton Roy "uvMonitor" spectrophotometer equipped with 254-nm photocell catridge. Purification of the crude DMT-protected oligomers (see above) utilized a system with 25 mL/min pump heads, a Hamilton PRP-1 (0.7 × 30.5 cm) column, and the gradient described above. The analyses of the purified oligomers and their Pt reaction products employed the following conditions: system with 5 mL/min pump heads, a Rainin Microsorb C18 (0.46 × 25 cm) column, a gradient of 10–22% B in 18 min, ambient temperature, and a flow rate of 1 mL/min. Typical retention times were 12 min for d(TCTCGGTCTC) and 18–19 min for *cis*-Pt(NH_3)$_2$–, Pt(en)–, and *cis*-Pt($MeNH_2$)$_2$– adducts of d(TCTCGGTCTC).

Atomic Absorption Spectroscopy. Pt analyses of the three HPLC-purified oligomer adducts were performed on a Perkin-Elmer Model 460 spectrometer equipped with an HGA-2100 controller, a graphite furnace, and a platinum hollow-cathode lamp. Optimum parameters for 40-μL samples were as follows: drying cycle, 90 °C for 77 s; charring cycle, 1100 °C for 20 s; atomization cycle, 2700 °C for 8 s. For each adduct, one Pt per strand was found, based on an ϵ_{260}(25 °C) value of 8800 M^{-1} cm^{-1}.

UV Spectroscopy. Melting experiments were performed with a Perkin-Elmer Lambda 3B spectrophotometer equipped with an electronically heated five-cell holder, temperature controller, and temperature programmer. The spectrophotometer was interfaced with an Apple IIe microcomputer that allowed for collection of absorbance vs temperature data directly.[30] An American Data Cable "Thermonitor" resistance measurement system utilizing a Yellow Springs Instruments Series 400 thermistor was employed for temperature measurements.

Five samples were run simultaneously in sealed cuvettes with a 1-cm path length. The first cuvette contained the reference buffer. The thermistor was placed in this cuvette to record sample temperature. Each of the remaining cuvettes contained solutions consisting of d(TCTCGGTCTC) (7.0 × 10^{-5} M bases), d(TCTCGGTCTC)–d(GAGACCGAGA) (6.4 × 10^{-5} M bases), or their Pt adducts in PIPES[10] 01

Figure 1. The 81.01-MHz ^{31}P NMR spectra of d(TCTCGGTCTC) at 25 °C, in 99.9% D_2O, and various Pt adducts: (a) no Pt, 0.050 M; (b) *cis*-Pt(NH_3)$_2$, 0.050 M; (c) Pt(en), 0.020 M; (d) *cis*-Pt($MeNH_2$)$_2$, 0.020 M.

(0.010 M PIPES, 0.010 M $NaNO_3$, 0.001 M EDTA,[22] pH 7.0) or PIPES 10 (0.010 M PIPES, 0.100 M $NaNO_3$, 0.001 M EDTA, pH 7.0) buffer. The temperature was increased at a rate of 0.5 °C/min. The temperature (5–95 °C) and absorbance values (~0.6 at 260 nm) were recorded every 2 min. In some cases, the solutions were allowed to cool to room temperature and solid $Mg(NO_3)_2$ was added to a final concentration of 0.1 M. The melting experiment was repeated.

The melting temperatures (T_m) of each oligomer and its Pt adduct were determined by calculation of $\Delta A/\Delta T$ were T_m is the temperature at which $\Delta A/\Delta T$ is a maximum. When the melting transition was broad, i.e., $\Delta A/\Delta T$ was linear, the midpoint of the transition is reported as the T_m.

Electrophoresis. Polyacrylamide gel electrophoresis was performed by using a described procedure[31] with gels containing one of the following: Tris–borate–EDTA (TBE) buffer (0.1 M Tris–borate (pH 8.3) and 0.2 mM EDTA) (low salt gel); Tris–borate–magnesium (TBM) buffer (0.1 M Tris–borate (pH 8.3) and 5 mM $MgCl_2$) (Mg gel); or TBE buffer with 6 M urea (denaturing gel). To prepare the gels, 0.15 mL of a 10% ammonium persulfate solution was added to 24 mL of 30% acrylamide (0.8 g of *N,N′*-methylenebis(acrylamide) + 30 g of acrylamide/100 mL of H_2O), 3.6 mL of TB (1 M Tris–borate, pH 8.3) buffer, 3.6 mL of 20 mM EDTA or 3.6 mL of 50 mM $MgCl_2$, and 4.8 mL of H_2O. Electrophoresis was carried out at 5 °C for ~12 h (TBE), ~24 h (TBM), or at ambient temperature for ~3 h (TBE–urea). Gels were stained with propidium iodide or acridine orange.

Results

^{31}P NMR Spectroscopy. *cis*-Pt(NH_3)$_2$[d(TCTCGGTCTC)-N7(5),N7(6)]. The ^{31}P NMR spectrum of a solution of d(TCTCGGTCTC) (25 °C, 0.050 M, and 99.9% D_2O) consists of two signals at −3.97 and −4.22 ppm, Figure 1a. Solid *cis*-Pt(NH_3)$_2$$Cl_2$ was added to a solution of this oligomer (0.001 M, pH 6.3) at a ratio of 1:1. After sitting at room temperature for 1 week, the reaction mixture was lyophilized and analyzed. HPLC results indicate the presence of only one product. The ^{31}P spectrum of *cis*-Pt(NH_3)$_2$[d(TCTCGGTCTC)-N7(5),N7(6)] (25 °C, 0.040 M, and 99.9% D_2O) exhibits a cluster of signals in the normal region (three resonances at −3.97, −4.05, and −4.22 ppm at a ratio of 2:1:2), but it also has four signals outside this region (downfield at −2.60 and −3.10 ppm and upfield at −4.64 and −4.77 ppm

(27) Sklenar, V.; Miyashiro, H.; Zon, G.; Miles, H. T.; Bax, A. *FEBS Lett.* **1984**, *208*, 94.
(28) Sklenar, V.; Bax, A. *J. Am. Chem. Soc.* **1987**, *109*, 7525.
(29) Jeener, J.; Meier, B. H.; Bachmann, P.; Ernst, R. R. *J. Chem. Phys.* **1979**, *71*, 4546.
(30) Reily, M. D. Ph.D. Thesis, Emory University, Atlanta, GA, 1987.
(31) Maniatis, T.; Jeffery, A.; van deSande, H. *Biochemistry* **1975**, *14*, 3787.

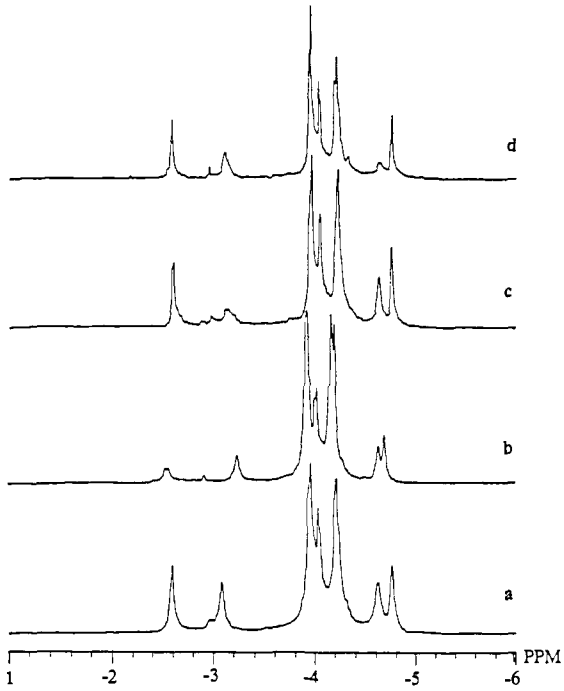

Figure 2. The 81.01-MHz ^{31}P NMR spectra of ^{17}O-labeled and unlabeled *cis*-$Pt(NH_3)_2$[d($T_1C_2T_3C_4G_5G_6T_7C_8T_9C_{10}$)]: (a) no label; (b) G_5-[^{17}O]G_6; (c) C_2[^{17}O]T_3; (d) T_3[^{17}O]C_4. Note that these spectra were recorded on four different samples. The spectra are somewhat sensitive to conditions, accounting for the slight difference in appearance and shifts in b.

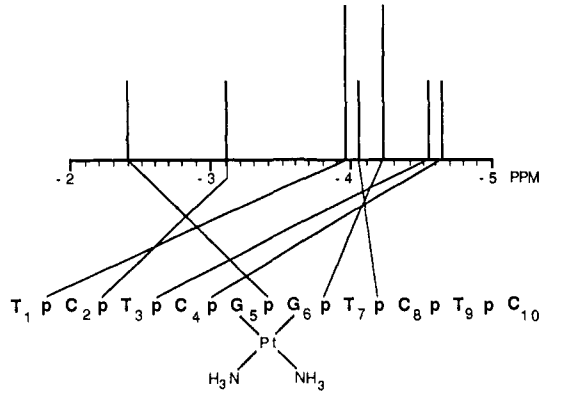

Figure 3. Schematic representation of the assignments of the ^{31}P NMR signals of *cis*-$Pt(NH_3)_2$[d(TCTCGGTCTC)-N7(5),N7(6)].

(Figure 1b)). Identical results with this platinated oligonucleotide have been reported previously.[7]

Assignments by ^{17}O Labeling. Five of the nine possible ^{17}O-labeled *cis*-$Pt(NH_3)_2$[d($T_1pC_2pT_3pC_4pG_5pG_6pT_7pC_8pT_9pC_{10}$)-N7(5),N7(6)] oligomers were synthesized. From the decrease in five ^{31}P NMR resonances (Figure 2) the following assignments were made: T_1pC_2 at −3.97 ppm, C_2pT_3 at −3.19 ppm, T_3pC_4 at −4.59 ppm, G_5pG_6 at −2.60 ppm, and T_7pC_8 at −4.05 ppm. den Hartog et al.[7] had previously assigned C_4pG_5, G_5pG_6, and G_6pT_7 via selective irradiation of H3′ resonances to signals that correspond to those at −4.74, −2.60, and −4.22 ppm, respectively, in our spectra. Thus, the $T_3pC_4pG_5$ fragment produces the two upfield signals, whereas C_2pT_3 and G_5pG_6 produce downfield signals (Figure 3). *All of the unusually shifted ^{31}P signals arise from groups 5′ to G_6.*

Temperature. The ^{31}P spectrum of *cis*-$Pt(NH_3)_2$[d(TCTCGGTCTC)-N7(5),N7(6)] is dramatically temperature sensitive.[7] On the basis of our new assignments, the most temperature-sensitive signals are the downfield C_2pT_3 signal and the upfield T_3pC_4 signal (Table SI). When the temperature was raised from 15 to 70 °C, the C_2pT_3 peak shifted upfield and the T_3pC_4 peak moved downfield into the normal range. The downfield

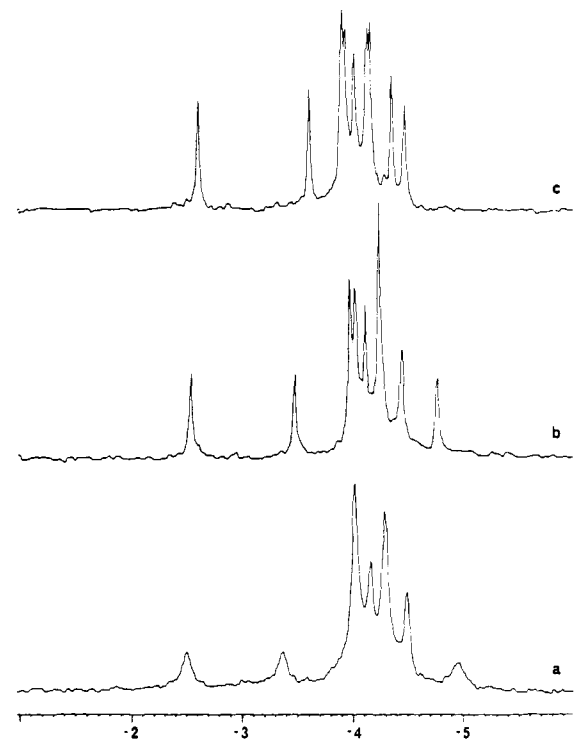

Figure 4. The ^{31}P NMR spectra of Pt(en)[d(TCTCGGTCTC)-N7(5),N7(6)], 0.020 M, at various temperatures: (a) 8 °C; (b) 25 °C; (c) 45 °C.

G_5pG_6 and upfield C_4pG_5 signals are affected to a lesser extent. They broadened slightly and shifted closer to the main signal but remained distinct at 70 °C.

Pt(en)[d(TCTCGGTCTC)-N7(5),N7(6)] and *cis*-Pt-$(MeNH_2)_2$[d(TCTCGGTCTC)-N7(5),N7(6)]. The ^{31}P NMR spectra of both the Pt(en) and *cis*-$Pt(MeNH_2)_2$ adducts exhibit the same pattern as the *cis*-$Pt(NH_3)_2$ adduct (Figure 1b). This similarity is strong evidence that these species also cross-link G_5 and G_6 by binding to N7. The ^{31}P NMR spectrum of Pt(en)[d-(TCTCGGTCTC)-N7(5),N7(6)] at 25 °C consists of two downfield signals at −2.53 and −3.46 ppm, two upfield peaks at −4.40 and −4.76 ppm, and four resonances between −3.9 and −4.2 ppm, Figure 1c. All peaks are sharp. The spectrum of *cis*-Pt-$(MeNH_2)_2$[d(TCTCGGTCTC)-N7(5),N7(6)] has two peaks downfield at −2.93 and −3.45 ppm, two peaks upfield at −4.36 and −4.69 ppm, and three resonances in the main signal, Figure 1d. The signals at −3.45 and −4.69 ppm are broad at 25 °C.

Reaction of $Pt(en)Cl_2$ and *cis*-$Pt(MeNH_2)_2Cl_2$ with d-(TCTCGGTCTC) ^{17}O-labeled at C_2pT_3 and G_5pG_6 allowed assignments (at 25 °C) of G_5pG_6 (−2.53 ppm) and C_2pT_3 (−3.46 ppm) for the Pt(en) adduct, and G_5pG_6 (−2.93 ppm) and C_2pT_3 (−3.45 ppm) for the *cis*-$Pt(MeNH_2)_2$ adduct; these results are consistent with assignments for the *cis*-$Pt(NH_3)_2$ adduct.

Temperature Effects. For Pt(en)[d(TCTCGGTCTC)-N7(5),N7(6)] at 8 °C, there were four ^{31}P signals observed outside of the main signal at −2.49, −3.35, −4.48, and −4.95 ppm, Figure 4. The signals at −2.49, −3.35, and −4.95 ppm were broad. When the temperature was raised to 15 °C, the signals at −3.35 (C_2pT_3) and −4.95 shifted 0.07 ppm upfield and downfield, respectively, and sharpened. The −2.49 ppm signal also sharpened. As the temperature was raised from 15 to 45 °C, the most dramatic effect was the 0.41 ppm downfield shift of the furthest upfield peak. The remaining upfield and two downfield signals shifted slightly toward the main signal area. The ^{31}P spectrum of *cis*-$Pt(MeNH_2)_2$[d-(TCTCGGTCTC)-N7(5),N7(6)] at 8 °C has broader signals than those of the other adducts. Raising the temperature above 25 °C sharpened all signals (Table SII in the supplementary material (see the paragraph at the end of the article)).

[*cis*-$Pt(NH_3)_2$[d(TCTCGGTCTC)-N7(5),N7(6)]]-d(GAGACC-GAGA). To *cis*-$Pt(NH_3)_2$[d(TCTCGGTCTC)-N7(5),N7(6)] was

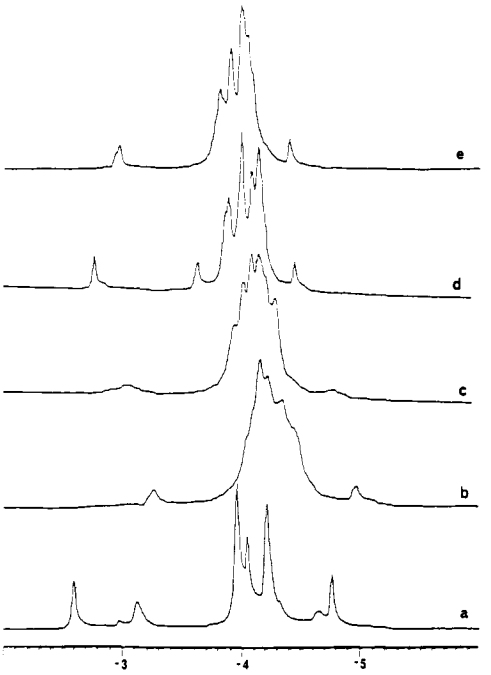

Figure 5. The ^{31}P NMR spectra of ^{17}O-labeled *cis*-Pt$(NH_3)_2$[d-(TCTCGGTCTC)-N7(5),N7(6)] (a) at 25 °C, and after addition of ~1 equiv of d(GAGACCGAGA) at various temperatures: (b) 13 °C; (c) 30 °C; (d) 50 °C; (e) 70 °C.

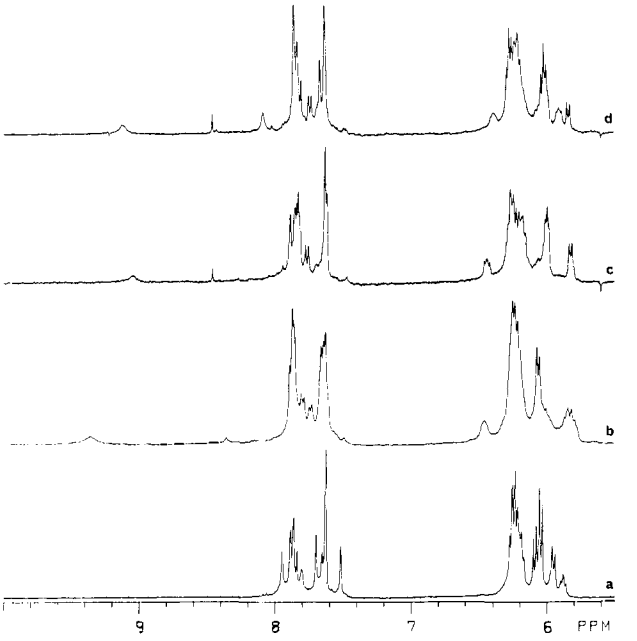

Figure 6. The ^1H NMR spectra of d(TCTCGGTCTC) at 25 °C, in 99.9% D_2O, and various Pt adducts: (a) no Pt, 0.050 M; (b) *cis*-Pt$(NH_3)_2$, 0.050 M; (c) Pt(en), 0.020 M; (d) *cis*-Pt$(MeNH_2)_2$, 0.020 M. Concentration values are base concentrations. D_2O impurity is present at 8.47 ppm.

added 0.6 equiv of the complementary strand, d(GAGACCGAGA), and the ^{31}P NMR spectrum was obtained at 20 °C. Three signals are observed in the downfield region. Two are of approximately the same intensity and occur at ca. −2.6 and −3.1 ppm, chemical shift values of platinated single-strand signals. A third signal occurs at −3.2 ppm, the chemical shift value reported by den Hartog et al.[7] for the platinated duplex structure. These results demonstrate that ^{31}P NMR spectroscopy may be used to verify the stoichiometry of platinated d(TCTCGGTCTC) to its complementary strand.

To separate solutions of *cis*-Pt$(NH_3)_2$[d(TCTCGGTCTC)-N7(5),N7(6)] (PIPES 10) labeled with ^{17}O at C_2pT_3 or at T_3pC_4, a solution with 0.95 equiv of d(GAGACCGAGA) was added. The resulting ^{31}P spectrum at 13 °C exhibited one downfield and one upfield signal (−3.2 and −4.9 ppm) with equal intensities (Figure 5b). Identical results were obtained by den Hartog et al.,[7] who assigned these signals as G_5pG_6 and C_4pG_5, respectively. The G_5pG_6 signal was assigned on the basis of an H3′–^{31}P selective irradiation experiment. The C_4pG_5 signal was assigned on the basis of ^{31}P chemical shift temperature-dependency results.[7] The chemical shift of the −4.9 ppm signal was monitored as a function of temperature. At $T > 60$ °C, the shift of this signal coincided with the signal assigned as C_4pG_5 in the platinated single strand. An additional signal moved downfield out of the normal range at 45 °C and then returned to the normal range at 70 °C.[7] The chemical shift of this signal is similar to the C_2pT_3 signal of the platinated single strand in this temperature range.

We conducted the same study and found that, in addition to the chemical shift changes found by den Hartog et al.,[7] broadening occurs upon raising the temperature (Figure 5). As the temperature was raised to 30 °C, the two unusually shifted signals broadened almost into the base line. Between 30 and 50 °C, they began to sharpen and both moved downfield. Severe signal broadening makes it difficult to follow the position of these signals as a function of temperature. Assignments made by den Hartog et al.[7] on the basis of chemical shift temperature-dependency results can, therefore, be only tentative. We have, however, found that ^{17}O labeling at C_2pT_3 or at T_3pC_4 had no detectable effect on the intensity of the downfield or the upfield signal of the platinated duplex. If it is assumed that two of the four unusually shifted ^{31}P signals of *cis*-Pt$(NH_3)_2$[d(TCTCGGTCTC)-N7(5),-N7(6)] remain outside of the normal region after duplexation, the resonances at −3.2 and −4.9 ppm of [*cis*-Pt$(NH_3)_2$[d-(TCTCGGTCTC)-N7(5),N7(6)]–d(GAGACCGAGA) can be assigned to G_5pG_6 and C_4pG_5, respectively. These results support the assignments made by den Hartog et al.[7]

^1H NMR Spectroscopy. *cis*-Pt$(NH_3)_2$[d(TCTCGGTCTC)-N7(5),N7(6)]. 3–0 ppm Region. Progress of the reaction of d(TCTCGGTCTC) with *cis*-Pt$(NH_3)_2Cl_2$ may be monitored by observing the four thymine methyl ^1H NMR signals at 1.70, 1.82, 1.84, and 1.88 ppm. As the reaction proceeds, the most upfield resonance at 1.70 ppm disappears while a new downfield signal at 1.97 ppm emerges. This signal is assigned at T_7Me by 2D NOE methods (see below). New resonances are also observed at 1.83 (two signals) and 1.87 ppm, but it is less convenient to monitor the reaction progress in this crowded region.

10–7 ppm Region. The change in ^1H NMR spectrum of d-(TCTCGGTCTC) (Figure 6a) on formation of *cis*-Pt$(NH_3)_2$[d-(TCTCGGTCTC)-N7(5),N7(6)] (Figure 6b, 25 °C, pH 6.8, 0.050 M) is similar to that observed by den Hartog et al.,[16] who made the following assignments: T_3 H6 (7.69 ppm), C_4 H6 (7.81 ppm), and T_7 H6 (7.92 ppm). The three C H6 signals occur in a crowded region at ca. 7.8 ppm. T_3 H6 and the two unassigned T H6 signals also severely overlap. A broad resonance at 9.37 ppm was assigned by den Hartog et al. to G_6 H8 on the basis of 1D NOE results. They also observed a broad peak downfield at 8.1 ppm (32 °C) and assigned it to G_5 H8. At 25 °C, we observe the G_6 H8 but not the G_5 H8 peak.

15–12 ppm Region. No signals were found in this region for *cis*-Pt$(NH_3)_2$[d(TCTCGGTCTC)-N7(5),N7(6)] (6 °C, pH 6.8, 0.040 M, 10% D_2O), indicating that no stable base pairs are present.

Temperature Dependence. At 5 °C, the ^1H NMR spectrum of *cis*-Pt$(NH_3)_2$[d(TCTCGGTCTC)-N7(5),N7(6)] (pH 6.8, 0.040 M) has fairly broad signals (Figure 7). In particular, the G_6 H8 signal had broadened into the base line. As the temperature was increased to 45 °C, all signals sharpened. At ~53 °C, a fairly broad signal began to move downfield out of the aromatic signal cluster (8.0–7.4 ppm). This signal is assigned as G_5 H8 on the basis of NOESY results (see below). In this temperature range (25–53 °C), G_6 H8 shifted upfield to 9.22 ppm and T_7 H6 shifted upfield to 7.84 ppm. When the temperature was raised further to 70 °C, the G_6 H8, G_5 H8, and T_7 H6 signals moved to 9.07, 8.08, and 7.75 ppm, respectively. All signals broadened, except

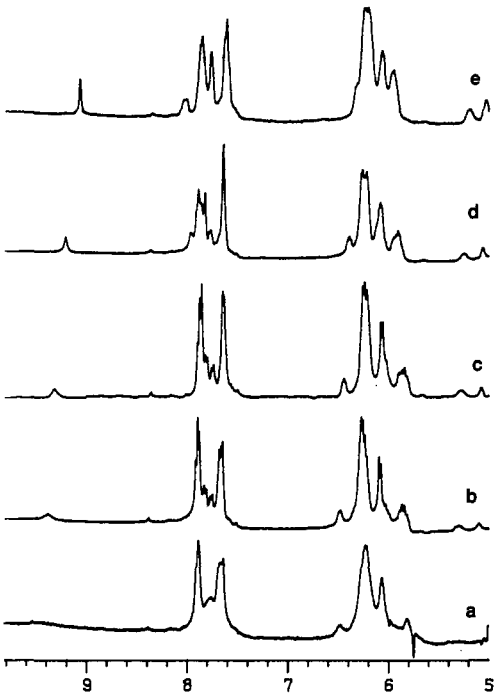

Figure 7. The ^{1}H NMR spectra of *cis*-Pt$(NH_3)_2${d(TCTCGGTCTC)-N7(5),N7(6)}, 0.040 M, at various temperatures: (a) 5 °C; (b) 25 °C; (c) 35 °C; (d) 53 °C; (e) 70 °C.

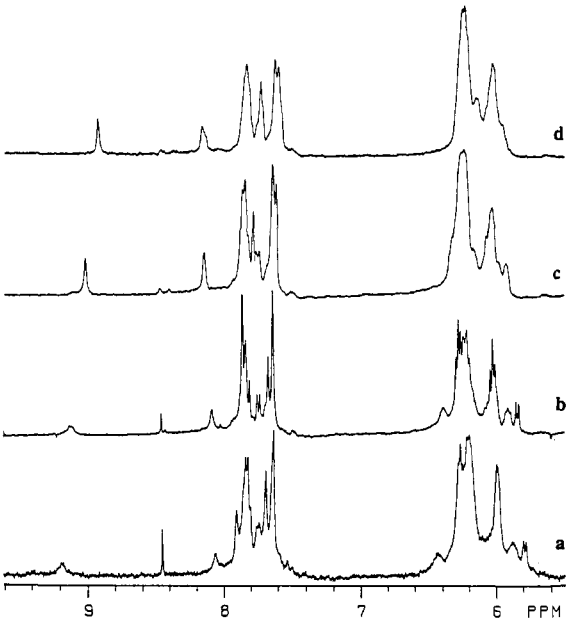

Figure 8. The ^{1}H NMR spectra of *cis*-Pt$(MeNH_2)_2${d-(TCTCGGTCTC)-N7(5),N7(6)}, 0.020 M, at various temperatures: (a) 5 °C; (b) 25 °C; (c) 45 °C; (d) 70 °C. D_2O impurity is present at 8.47 ppm.

for G_6 H8, which continued to sharpen.

Addition of Cu$(NO_3)_2$. Aliquots of a 0.01 M Cu$(NO_3)_2$ solution in D_2O were added to a solution of *cis*-Pt$(NH_3)_2${d-(TCTCGGTCTC)-N7(5),N7(6)} (0.050 M, pH 5.9) containing a trace amount of EDTA until a small amount of broadening could be detected in the H1′/H5 signals (6.6–5.6 ppm). From this point, the ^{1}H NMR spectrum of the adduct was observed upon titration with 0.01 M Cu$(NO_2)_2$, Figure 9. This titration was conducted at 55 °C to be able to observe the G_5 and G_6 H8 signal. The N7 of typical oxopurine residues are accessible to Cu^{2+}, which readily broadens the H8 signal.[32,33] Platination eliminates this accessibility, and the H8 signal remains even at high Cu^{2+} concentrations.[33] Even at a high Cu^{2+} concentration (9.4×10^{-4} M), the G_5 and G_6 H8 signals are still present, thus providing additional evidence for Pt binding of G_5 and G_6 at N7. The T H6 signals were also unaffected due to lack of Cu^{2+} binding to T residues.[32,33] All C H6 resonances were broadened considerably at 5×10^{-4} M Cu^{2+}. The C H5 signals disappeared at 1.6×10^{-4} M.

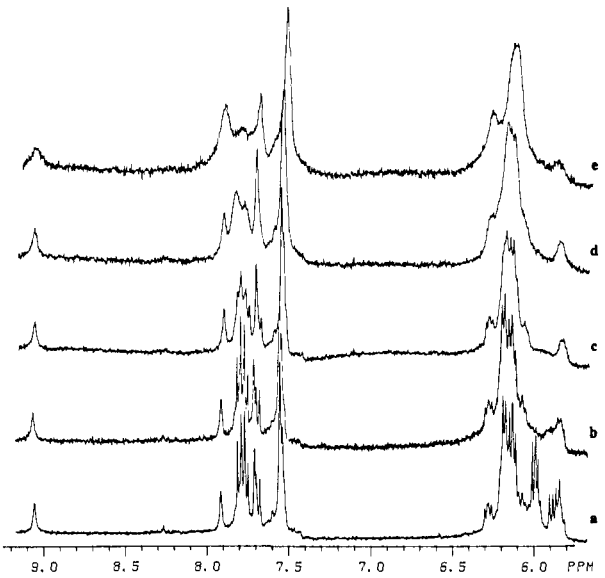

Figure 9. Effect of Cu$(NO_3)_2$ on the ^{1}H NMR spectrum of *cis*-Pt$(NH_3)_2${d(TCTCGGTCTC)-N7(5),N7(6)} (55 °C, pH 5.9, D_2O, 0.050 M). Cu^{2+} concentrations are as follows: (a) 5×10^{-5}, (b) 6×10^{-5}; (c) 1.6×10^{-4}; (d) 3.8×10^{-4}; (e) 9.4×10^{-4} M.

Pt(en){d(TCTCGGTCTC)-N7(5),N7(6)} and *cis*-Pt$(MeNH_2)_2${d(TCTCGGTCTC)-N7(5),N7(6)}. 3–0 ppm Region. The ^{1}H spectra of the Pt(en) and *cis*-Pt$(MeNH_2)_2$ adducts both exhibit a methyl peak at 1.97 ppm, analogous to the T_7 Me signal of the *cis*-Pt$(NH_3)_2$ adduct. The Pt(en) adduct has three methyl resonances at 1.80, 1.83, and 1.85 ppm. The *cis*-Pt$(MeNH_2)_2$ adduct has signals at 1.83, 1.86, and 1.88 ppm.

10–7 ppm Region. In this region, the ^{1}H NMR spectra of all three adducts are similar. In the spectrum of the Pt(en) adduct (25 °C, pH 6.8, 0.020 M, Figure 6c), a peak observed slightly downfield may be the H8 of G_5. A broad signal at 9.0 ppm, analogous to that seen at 9.4 ppm for the *cis*-Pt$(NH_3)_2$ adduct, is assigned to the H8 of G_6. In the spectrum of *cis*-Pt$(MeNH_2)_2${d(TCTCGGTCTC)-N7(5),N7(6)}, a downfield signal is observed at 8.1 ppm (Figure 6d), probably the H8 of G_5. The signal corresponding to the H8 of G_6 occurs at 9.1 ppm and, like that of the other Pt adducts, is fairly broad.

Temperature Dependence. The behavior of aromatic signals of *cis*-Pt$(MeNH_2)_2${d(TCTCGGTCTC)-N7(5),N7(6)} upon temperature variation was similar to that of the *cis*-Pt$(NH_3)_2$ adduct (Figure 8). The G_6 H8 signal shifted upfield and the G_5 H8 signal shifted downfield as the temperature was raised. All signals sharpened upon temperature increase. However, about 53 °C, all signals began to broaden except for G_6 H8, which continued to sharpen.

[*cis*-Pt$(NH_3)_2${d(TCTCGGTCTC)-N7(5),N7(6)}]-d(GAGACCGAGA). 10–7 ppm Region. The ^{1}H NMR spectrum of the duplex (0.090 M, pH 7.0) at 25 °C (Figure 10b) closely resembles that previously reported.[16] A signal at 8.78 ppm has been assigned to the G_5 H8.[16] The assigned G_6 H8 signal is observed further upfield at ~8.0 ppm, and, upon going from the platinated single strand to the duplex, the two G H8 signals exchange relative positions.[16]

15–12 ppm Region. For a solution of [*cis*-Pt$(NH_3)_2${d-(TCTCGGTCTC)-N7(5),N7(6)}-d(GAGACCGAGA) (PIPES 10, pH 6.8) we observed the same imino spectrum as den Hartog

(32) Berger, N. A.; Eichhorn, G. L. *J. Am. Chem. Soc.* **1971**, *93*, 7062.

(33) Reily, M. D.; Marzilli, L. G. *J. Am. Chem. Soc.* **1985**, *107*, 4916.

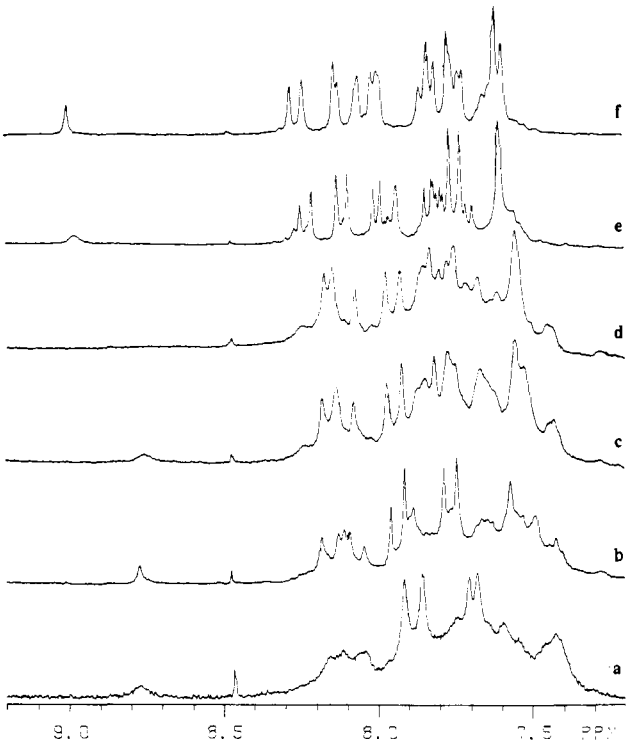

Figure 10. The ^{1}H NMR spectra of *cis*-Pt$(NH_3)_2${d-(TCTCGGTCTC)-N7(5),N7(6)} after addition of d(GAGACCGAGA) to a total ratio of 100:95, respectively, at various temperatures: (a) 5 °C; (b) 25 °C; (c) 35 °C; (d) 40 °C; (e) 57 °C; (f) 70 °C.

et al.,[17] who have assigned the resonances on the basis of the melting behavior and 1D NOE experiments.

Temperature Dependence. For a solution of [*cis*-Pt$(NH_3)_2${d-(TCTCGGTCTC)-N7(5),N7(6)}-d(GAGACCGAGA) (0.050 M base pair, PIPES 10, pH 6.8), some shifting occurs within the main signal between 25 and 70 °C (Figure 10). The large number of signals in this region makes it difficult to follow the shifting of individual signals. The most dramatic effect observed upon raising the temperature is that upon the G_5 H8 signal at 8.78 ppm (at 25 °C). At 30 °C, this signal began to broaden and by 45 °C disappeared into the base line. Little shift in position was observed during the process. The temperature was increased further, and at 60 °C, a new fairly broad signal appeared at 9.0 ppm; at 70 °C, this signal sharpened.

^{195}Pt NMR Spectroscopy. The environment of the Pt moiety[34,35] was investigated by ^{195}Pt NMR spectroscopy. The ^{195}Pt NMR spectrum of a solution of *cis*-Pt$(NH_3)_2${d(TCTCGGTCTC)-N7(5),N7(6)} revealed a signal at −2450 ppm. This chemical shift is similar to shifts reported for *cis*-Pt$(NH_3)_2$ compounds with two guanine bases bound via N7.[34]

Two-Dimensional NMR Spectroscopy. *cis*-Pt$(NH_3)_2${d-(TCTCGGTCTC)-N7(5),N7(6)}. den Hartog et al.[7,16] had previously assigned resonances at 5.28 and 5.06 ppm (32 °C) as H3′ signals of G_5 and G_6, respectively, via 1D NOE irradiation experiments. C_4 and C_{10} H3′ signals were also assigned. A selective reverse chemical shift correlation (SRCSC)[27,28] experiment was conducted with *cis*-Pt$(NH_3)_2${d(TCTCGGTCTC)-N7(5),N7(6)} (0.030 M, pH 7.0, 99.96% D_2O) at 32 °C (Figure 11). Eight cross peaks between ^{31}P signals and signals of the H3′ protons 5′ to the phosphate group were observed. By identifying the H3′ signal coupled to a previously assigned ^{31}P signal (^{17}O labeling), we were able to confirm two previous H3′ assignments[7,16] and identify three additional H3′ signals, Table I. A cross peak between the C_4pG_5 signal (−4.70 ppm) and a ^{1}H signal at 4.61 ppm confirmed the assignment of C_4 H3′. Cross peaks with assigned ^{31}P NMR resonances assigned other H3′ signals as C_2

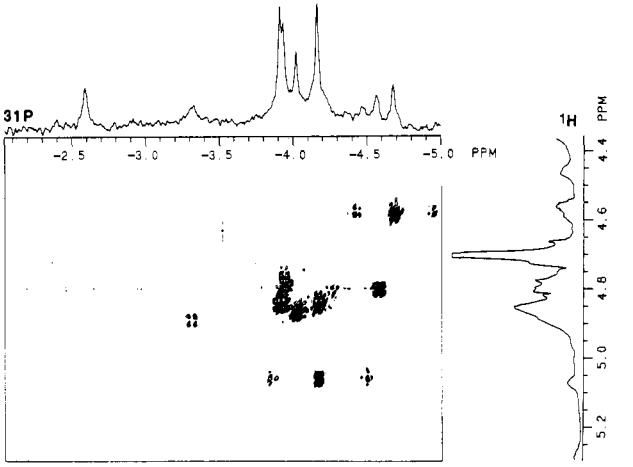

Figure 11. Contour plot of ^{1}H-detected ^{1}H–^{31}P selective reverse chemical shift correlation experiment of *cis*-Pt$(NH_3)_2${d(TCTCGGTCTC)-N7(5),N7(6)} (0.030 M, 10^{-4} M EDTA, pH 7, 32 °C). Normal 1D ^{1}H and ^{31}P spectra are shown along respective axes for reference. Spectral conditions are given in the experimental section.

Table I. Measured Chemical Shift and Coupling Constant Values and Estimated Dihedral and Torsional Angle Values for *cis*-Pt$(NH_3)_2${d(TCTCGGTCTC)-N7(5),N7(6)} at 32 °C

phosphate	H3′ chem[a] shift, ppm	^{31}P chem shift, ppm	$^3J_{H3'-P}$, Hz	ϕ_{PH},[b] deg	ϵ,[c] deg
$T_{1p}C_2$	4.81[d]	−3.98	7.0[e,f]	34	206
$C_{2p}T_3$	4.88	−3.24	8.9[e]	23	217
$T_{3p}C_4$	4.82	−4.54	8.0[e]	29	211
$C_{4p}G_5$	4.61[g]	−4.70	7.1[e]	34	206
$G_{5p}G_6$	5.28[g]	−2.61	8.9[h,i]	23	217
$G_{6p}T_7$	5.08[g]	−4.22	5.8[h]	39	201
$T_{7p}C_8$	4.89	−4.05	7.0[e]	34	206
$C_{8p}T_9$	4.8[d]	ca. −4.0	7.0[e,f]	34	206
$T_{9p}C_{10}$	4.8[d]	ca. −4.0	7.0[e,f]	34	206
C_{10}	4.56[g,j]				

[a] Except where indicated, assignments are based on results of selective reverse chemical shift correlation experiment at 32 °C. [b] Estimated as described in the text. $^3J_{H3'-P} = 15.3\cos^2\phi_{PH} - 6.1\cos\phi_{PH} + 1.6$.[43] [c] Estimated from $\phi_{PH}(\epsilon^t = 240° - \phi_{PH})$. [d] Signal must be at 4.81 or 4.85 ppm, but specific assignment cannot be made. [e] Value from results of SRCSC experiment. [f] The ^{31}P NMR signal is not assigned. However, the three possible signals all have $^3J_{H3'-P}$ values of approximately 7.0 Hz. [g] Assignments by den Hartog et al.[14,15] [h] Value measured from results of 2D J experiment. [i] Intensity observed in 2D J experiment at 32 °C was too low to measure coupling. The value listed was measured at 40 °C. [j] Assignment not possible by SRCSC experiment due to lack of 3′ phosphate group.

(4.88 ppm), T_3 (4.82 ppm), and T_7 (4.89 ppm). The C_2p cross peaks was weak. The downfield G_5pG_6 and G_5 H3′ signals exhibit no cross peak to each other. The ^{31}P NMR signals at −3.9 and −4.2 ppm each contain resonances from two phosphate groups. The signal at −4.2 ppm contains the G_6pT_7 resonance and has two cross peaks to H3′ signals, one of which was assigned to G_6 H3′.[7,15] The other cross peak is to a H3′ at 4.85 ppm. The −3.9 ppm ^{31}P signal contains the T_1pC_2 resonance and exhibits two cross peaks at 4.81 and 4.85 ppm, one of which must be T_1 H3′.

$^3J_{H3'-P}$ values were measured for *cis*-Pt$(NH_3)_2${d-(TCTCGGTCTC)-N7(5),N7(6)} from 2D J experiments[28] at 32, 40, and 48 °C (Table I). In this experiment, we detected coupling for G_5p of 8.6 Hz at 48 °C and 8.9 Hz at 40 °C, but the cross peak was unusually broad (2 Hz) and the intensity was low (Figure SI, supplementary material). At 32 °C, the signal intensity was too low to measure the coupling. The following $^3J_{H3'-P}$ values were measured for G_6p: 5.7 Hz (32 °C), 5.9 Hz (40 °C), and 5.8 Hz (48 °C). C_4p coupling was difficult to detect in this experiment due to its H3′ position near the HDO signal, and overlap of H3′ signals made the measurement of the other six H3′–P couplings very difficult. These seven $^3J_{H3'-P}$ values were obtained from the SRCSC experiment (H3′ signals are dispersed) at 32 °C, Table

(34) Miller, S. K.; Marzilli, L. G. *Inorg. Chem.* **1985**, *24*, 2421.
(35) Marzilli, L. G.; Hayden, Y.; Reily, M. D. *Inorg. Chem.* **1986**, *25*, 974.

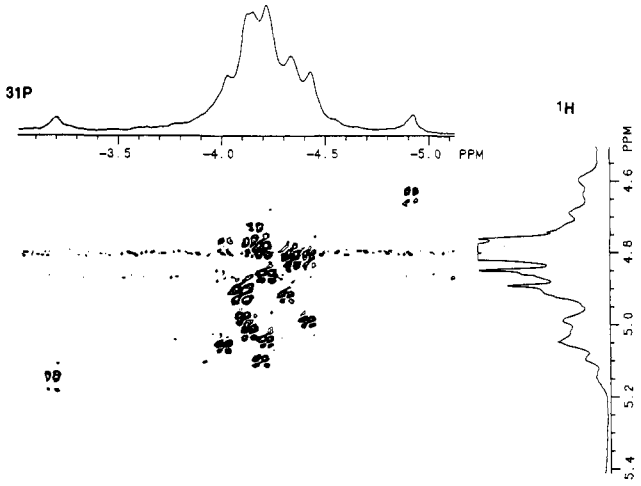

Figure 12. Contour plot of ^{1}H-detected ^{1}H–^{31}P selective reverse chemical shift correlation experiment of [*cis*-Pt(NH_3)$_2$[d(TCTCGGTCTC)-N7(5),N7(6)]]–d(GAGACCGAGA) (0.040 M, PIPES 10, pH 7, 22 °C). Normal 1D ^{1}H and ^{31}P spectra are shown along respective axes for reference. Spectral conditions are given in the Experimental Section.

I. If it is assumed that the ϵ(180 °C) range is predominant for the C4′–C3′–O3′–P torsional angle (see Discussion), ϕ_{PH},[36] and subsequently ϵ^t,[36] may be calculated by using the measured $^3J_{H3'-P}$ values and the Karplus relationship (see Discussion and Table I).

A 2D NOE experiment was conducted on *cis*-Pt(NH_3)$_2$[d(TCTCGGTCTC)-N7(5),N7(6)] at 32 °C. Because of the flexibility of the single strand and the number of overlapping signals in the aromatic, H1′, and methyl regions, few NOE cross peaks were observed. Some weak CH:H3′ NOEs were observed. A cross peak between G_5 H3′ and a broad signal at 7.88 ppm, slightly downfield of the main aromatic region, supports the assignment of this signal as G_5 H8.[16] Two NOEs are observed between C and T H6 (7.81 and 7.63 ppm) signals and H3′ signals at 4.89 and 4.88 ppm. However, due to the ambiguous assignments of some H3′ signals, no assignments of these H6 signals can be made.

A very weak NOE is observed between the T H6 and H1′ signals assigned as T_7.[16] An NOE between the T_7 H6 and a methyl signal at 1.98 ppm assigns this signal as T_7 Me. The three T H6 signals at 7.61 to 7.66 ppm and three T methyl signals at 1.82 to 1.87 ppm are so closely spaced that only one overlapping cross peak is observed. C H6 signals at 7.85 and 7.83 ppm exhibit overlapping NOEs to C H5 signals at 6.03 and 6.04 ppm, respectively. C H6 signals at 7.72 ppm (assigned as C_4[16]) and 7.81 ppm each have cross peaks with C H5 signals at 5.89 and 5.83 ppm, respectively.

[*cis*-Pt(NH_3)$_2$[d(TCTCGGTCTC)-N7(5),N7(6)]]–d(GAGACCGAGA). A SRCSC experiment was conducted with [*cis*-Pt(NH_3)$_2$[d(TCTCGGTCTC)-N7(5),N7(6)]–d(GAGACCGAGA) (0.040 M, PIPES 10, pH 7.0) at 22 °C (Figure 12). In addition to cross peaks between normal range ^{31}P signals and H3′ signals, connectivities were observed between the unusually shifted G_5pG_6 and C_4pG_5 ^{31}P signals and H3′ signals at 5.14 and 4.64 ppm, respectively. $^3J_{HCOP}$ values measured for G_5p and C_4p from this experiment were 9.0 and 6.7 Hz, respectively. ϕ_{PH} and ϵ^t were then calculated by using the measured $^3J_{HCOP}$ values and the Karplus relationship. For G_5p, ϕ_{PH} = 22° and ϵ^t = 218°. For C_4p, ϕ_{PH} = 36° and ϵ^t = 204°.

UV Spectroscopy. The melting behavior of d(TCTCGGTCTC), d(TCTCGGTCTC)–d(GAGACCGAGA), and their *cis*-Pt(NH_3)$_2$ adducts was investigated (Table SIII, supplementary material). In low salt buffer (0.010 M $NaNO_3$), both d(TCTCGGTCTC) and its Pt adduct exhibited little change in absorbance at 260 nm from 3 to 82 °C, but under high salt conditions (0.10 M $NaNO_3$), the absorbance of both species increased with temperature. The absorbance of d(TCTCGGTCTC) increased linearly from 3 to 55 °C and then more sharply from 55 to 75 °C. *cis*-Pt(NH_3)$_2$[d(TCTCGGTCTC)-N7(5),N7(6)] exhibited a small linear absorbance increase over the range 3–75 °C.

Under low salt conditions (0.010 M $NaNO_3$), d(TCTCGGTCTC)–d(GAGACCGAGA) exhibited a sharp transition with a T_m of 37 °C, a type of transition characteristic of the disruption of a duplex structure.[37] The transition was sharper and had a higher T_m (47 °C) at 0.1 M $NaNO_3$. The platinated duplex was less stable (T_m = 16 °C, low salt; 26 °C, high salt).

Addition of 0.1 M $Mg(NO_3)_2$, known to stabilize a DNA helix,[38] to 0.01 M $NaNO_3$ solutions of d(TCTCGGTCTC)–d(GAGACCGAGA) and *cis*-Pt(NH_3)$_2$[[d(TCTCGGTCTC)-N7(5),N7(6)]–d(GAGACCGAGA)] increased T_m to 52 and 30 °C, respectively. For the single strands in 0.1 M $Mg(NO_3)_2$ buffer, little or no change in absorbance was observed between 10 and 85 °C.

Electrophoresis. Polyacrylamide gel electrophoresis of the unplatinated and platinated single strand and duplex revealed one fluorescent band upon treatment with propidium iodide for each sample. Under low salt conditions (TBE buffer), the single-strand d(TCTCGGTCTC) had a greater mobility than that of the reference d(TCTCGGTCTC)–d(GAGACCGAGA) duplex (relative mobilities (RM) of 1.10 and 1.00, respectively). This result is consistent with findings that, for DNA smaller than 68 base pairs, single strands move faster than the duplexes from which they were derived.[31]

The positive charge of the Pt moiety should decrease the electrophoretic mobility for the Pt adducts. Platination of the single strand reduced the RM from 1.10 to 0.84. However, for the duplex, the RM actually increased slightly from 1.00 to 1.02. An explanation for this apparent lack of mobility change upon platination of d(TCTCGGTCTC)–d(GAGACCGAGA) may be destabilization or bending of the duplex (increase in mobility) offset by the positive charge addition (decrease in mobility).

On treatment with acridine orange, the bands of d(TCTCGGTCTC) and its Pt adduct gave a green fluorescence, indicative of a single-stranded form.[39] The bands of d(TCTCGGTCTC)–d(GAGACCGAGA) and its Pt adduct fluoresced red. This result indicates that even after platination, the duplex retains its double-stranded form.[39] Other groups have reached this same conclusion on the basis of NMR[15,16] results.

Under high salt conditions favoring the duplex form (TBM buffer), the difference in mobility between the single-strand d(TCTCGGTCTC) and the duplex d(TCTCGGTCTC)–d(GAGACCGAGA) increased (RM of 1.15 and 1.00, respectively). This effect may be due to stabilization of the duplex by Mg^{2+} resulting in a lower mobility for d(TCTCGGTCTC)–d(GAGACCGAGA). The mobility of the platinated duplex (RM = 0.99) remained essentially the same as for the unplatinated duplex. *cis*-Pt(NH_3)$_2$[d(TCTCGGTCTC)-N7(5),N7(6)] still exhibited a lower mobility than the other oligomers, although the difference was not quite so marked (RM = 0.91).

Under denaturing conditions, d(TCTCGGTCTC) and its Pt adduct exhibited similar mobility characteristics as under other conditions, i.e., platination produced a significant (24%) decrease in mobility. This result suggests that the platinated oligomer has an overall shape not grossly different from that of the parent single strand.

(36) In this case, ϕ_{PH} is defined as the angle between two planes formed by H3′–C3′–O3′ and by C3′–O3′–P. $^3J_{HCOP}$ is the same regardless of the direction of the angle (e.g., 30° vs −30° or 330°); therefore, the smallest possible positive value is reported. ϵ is defined as the angle between the two planes formed by C4′–C3′–O3′ and by C3′–O3′–P. ϵ = 0° when C4′ and P are eclipsed. The positive direction is obtained by moving the rear bond clockwise with respect to the front bond in the standard Newman projection. See ref 44 for further details.

(37) Markey, L. A.; Blumenfeld, K. S.; Kozlowski, S.; Breslauer, K. J. *Biopolymers* **1983**, *22*, 1247.
(38) Saenger, W. *Principles of Nucleic Acid Structures*; Springer-Verlag: New York, 1984; p 143.
(39) Simpkins, H.; Pearlman, L. F. *FEBS Lett.* **1984**, *169*, 30.

Discussion

As mentioned in the introduction, the unusual shifts of the ^{31}P NMR signals of *cis*-Pt$(NH_3)_2$\{d(TCTCGGTCTC)-N7(5),N7(6)\}, combined with the adduct's well-established composition and platination site, suggested it may be an excellent standard for a DNA single strand with conformational distortion induced by a metal ion. Although several initial conformations can be proposed and assessed with our results and those reported by den Hartog et al.,[7,16,17] we suggest, initially, models I and II as a framework for our discussion.

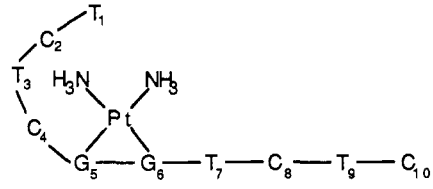

Model I

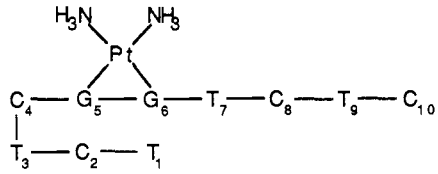

Model II

The primary reason for focusing on these two models is the ^{31}P NMR spectrum of *cis*-Pt$(NH_3)_2$\{d(TCTCGGTCTC)-N7(5),N7(6)\}. By observation of the ^1H spectrum under simultaneous selective irradiation of a ^{31}P resonance, the three ^{31}P signals were previously assigned.[7] However, six ^{31}P signals, including two outside the normal range, remained unassigned due to two drawbacks to the selective irradiation approach. First, unless one is dealing with a very small oligonucleotide, only the unusually shifted signals are adequately resolved for selective irradiation. Second, to assign the ^{31}P resonances, the H3′ resonances must be assigned. NOESY and/or COSY techniques can provide these assignments in theory. In practice, the H3′ signals can be overlapped, leading to ambiguity, and the flexibility of single strands may diminish both the number and intensity of NOE cross peaks.

^{31}P NMR spectra of *cis*-Pt$(NH_3)_2$\{d(TCTCGGTCTC)-N7(5),N7(6)\}, labeled at five phosphate groups with ^{17}O, confirmed the G_5pG_6 ^{31}P assignment[7] to the most downfield signal and identified four additional signals (Figure 3). The furthest upfield signal (−4.77 ppm, 25 °C) had been assigned to C_4pG_5.[7] The ^{17}O method allowed assignment of the remaining two signals outside the normal range as C_2pT_3 (−3.10 ppm, 25 °C) and T_3pC_4 (−4.64 ppm, 25 °C). Thus, the three phosphate groups with unusually shifted signals not directly attributable to Pt binding are all located in the 5′ direction of the Pt-bound G_5pG_6 site; consequently, models I and II were evaluated. Both models can explain normal shifts for T_1pC_2, G_6pT_7, T_7pC_8, C_8pT_9, and T_9pC_{10}.

Below 24 °C, there was little change in the ^{31}P NMR spectrum of *cis*-Pt$(NH_3)_2$\{d(TCTCGGTCTC)-N7(5),N7(6)\}.[7] Between 25 and 70 °C, three of the unusual signals shifted toward the normal range in a fairly linear, rather than sigmoidal, manner. The change in shift was greatest for the signals of C_2pT_3 and T_3pC_4, the two phosphate groups with unusual ^{31}P NMR signals that are furthest along the chain from the Pt binding site. Above 60 °C, the C_2pT_3 and T_3pC_4 ^{31}P signals were back in the normal range. Surprisingly, the C_4pG_5 signal remains outside the normal range even at 70 °C. The G_5pG_6 signal is only slightly temperature sensitive and remains shifted outside the normal range. This is typical of ^{31}P signals of phosphate groups between Pt-bound G residues.[12,19c]

Models I and II suggest that there can be considerable deviation in bond and torsion angles of C_2pT_3 and T_3pC_4. For either model, the hydrogen-bonding interactions (i.e., between NH_3 and the bases and/or phosphates in model I and between bases in model II) would be disrupted at high temperature. The C_4pG_5 stacking suggested by den Hartog et al.[16] will also diminish but may still be present at 70 °C, as evidenced by the upfield C_4pG_5 shift. Taken in isolation, the ^{31}P NMR results could support either model.

Four sets of results indicate that model I is more reasonable than either a hairpinlike compound found for *cis*-Pt(en)\{d(TATAGGGTACCCATA)\}[19] or model II. First, no signals typical of hydrogen-bonded imino protons are observed in the 15–12 ppm region, nor were any signals characteristic of loop regions observed at ~11 ppm. Such signals would be expected for a hairpinlike structure and, possibly, model II. Second, relatively few cross peaks, particularly internucleotide, were observed in 2D NOE experiments conducted at 15 and 32 °C. Such few cross peaks are uncharacteristic of spectra of hairpin or hairpinlike structures.[19] Third, electrophoresis (low salt, Mg, and denaturing conditions) shows a decrease in mobility of the oligomer upon platination. This decrease is presumably due to the positive charge contribution of the Pt moiety. Compact structures such as hairpins typically exhibit greater mobility than comparable duplex or single-strand structures.[40,41] Staining of the electrophoresis band corresponding to *cis*-Pt$(NH_3)_2$\{d(TCTCGGTCTC)-N7(5),N7(6)\} with acridine orange produced a green fluorescence, demonstrating a single-stranded structure.[39] These electrophoresis results are more easily understood with model I. Fourth, the UV absorbance of a solution of *cis*-Pt$(NH_3)_2$\{d(TCTCGGTCTC)-N7(5),N7(6)\} shows no increase from 20 to 70 °C (Table SIII, supplementary material). For model II, an increase in absorbance is expected with increasing temperature.

Considering the UV absorbance, ^{31}P NMR, and ^1H NMR data on *cis*-Pt$(NH_3)_2$\{d(TCTCGGTCTC)-N7(5),N7(6)\} (little or no salt solutions), it appears as though the platinated single strand undergoes a gradual disruption of the looped structure. At high temperature, distortion in the sugar phosphate backbone of G_5pG_6 due to Pt binding remains. Also, slight distortion in C_4pG_5 remains at high temperature possibly due to Pt amine–phosphate hydrogen bonding or CG stacking.

In order to further assess model I and its generality, we treated d(TCTCGGTCTC) with other Pt compounds. ^{31}P and ^1H NMR data indicate that the Pt(en) and *cis*-Pt$(MeNH_2)_2$ adducts have structures similar to the *cis*-Pt$(NH_3)_2$ adduct. The G_5pG_6 signal of *cis*-Pt(en)\{d(TCTCGGTCTC)-N7(5),N7(6)\} is only slightly downfield of the analogous signal for the *cis*-Pt$(NH_3)_2$ compound (Figure 4). However, the C_2pT_3 signal of the Pt(en) compound is much closer to the normal range. The ^{31}P NMR spectrum of *cis*-Pt$(MeNH_2)_2$\{d(TCTCGGTCTC)-N7(5),N7(6)\} exhibits a G_5pG_6 signal upfield by 0.33 ppm of the analogous signal of the *cis*-Pt$(NH_3)_2$ compound (Table SII, supplementary material). The C_2pT_3 signal occurs at the same chemical shift value as the Pt(en) compound (upfield of *cis*-Pt$(NH_3)_2$) but is very broad.

The difference in chemical shift of the C_2pT_3 signal and the different temperature dependence of one of the upfield ^{31}P NMR signals provide further evidence for model I. For this model, the nature of the amine ligand should influence the interaction. In model II, it is difficult to rationalize these differences in the ^{31}P NMR spectra of the adducts.

The differences in chemical shift of the G_5pG_6 signal among the three Pt adducts (Figure 6) suggest slight differences in structure. In a study of *cis*-PtA_2\{d(TGGT)-N7(2),N7(3)\},[12] the GpG shift follows the order (most downfield) en > *cis*-$(NH_3)_2$ > *cis*-$(MeNH_2)_2$. This trend was correlated with the potential hydrogen-bonding ability of the Pt moiety. We observed the same trend. The G_5pG_6 signal of the Pt(en) compound is slightly downfield of that of the *cis*-Pt$(NH_3)_2$ compound, which is downfield of that of the *cis*-Pt$(MeNH_2)_2$ compound.

Although such shift trends do not give direct evidence for such hydrogen bonding, molecular mechanics calculations of *cis*-Pt$(NH_3)_2$\{[d(TCTCGGTCTC)-N7(5),N7(6)]-d(GAGACCGA-

(40) Wemmer, D. E.; Benight, A. S. *Nucleic Acids Res.* **1985**, *13*, 8611.
(41) Germann, M. W.; Schoenwaelder, K.-H.; van de Sande, J. H. *Biochemistry* **1985**, *24*, 5698.

GA)}[13] and X-ray structures of *cis*-Pt$(NH_3)_2${d(pGpG)-N7(1),-N7(2)}[14] and *cis*-Pt$(NH_3)_2${d(CGG)-N7(2),N7(3)}[15] also suggest that hydrogen bonding between one amine ligand on Pt and the phosphate group 5′ to the dGpG moiety is an important feature of Pt binding.

The coupling constant $^3J_{H3'-P}$ is a function of the torsional angle ϕ_{PH}[36] in the following manner:[42]

$$^3J_{HCOP} = 15.3 \cos^2 \phi_{PH} - 6.1 \cos \phi_{PH} + 1.6$$

The three staggered conformations have a C4′–C3′–O3′–P torsional angle (ϵ)[36] with the following values and designations: ϵ^+ (60°), ϵ^t (180°), and ϵ^- (300°).[43] X-ray studies[44,45] and theoretical calculations[46] have indicated that only two of these rotamers occur, i.e., ϵ^t and ϵ^-. No evidence has been found for the existence of the ϵ^+ conformation.[45,47,48] In the ϵ^t and ϵ^- rotamers, the P atom occupies approximately symmetrical positions with respect to H3′, and it follows that $^3J_{H3'-P}$ cannot distinguish between the two. However, various studies have indicated that the position of the rotamer equilibrium about ϵ in ribose 3′-phosphates is correlated with the sugar ring N/S equilibrium, i.e., the N-type ribose ring is exclusively associated with the ϵ^t conformation, whereas the S-type ribose ring allows both the ϵ^t and the ϵ^- conformations.[49–55] Two ranges of $^3J_{H3'-P}$ values, one for RNA single strands[42,43] (8–10 Hz, ϵ = ~210°) and another for DNA single strands[43,56–58] (5–7 Hz, ϵ = ~180°), have been observed. RNA consists of predominantly N-type ribose rings, whereas DNA sugar rings are primarily S type.

Several studies have been conducted on the relationship of $^3J_{H3'-P}$ to sugar conformation and degree of stacking. First, an investigation of five oligomers that show a large shift of the N/S equilibrium with temperature revealed an increase in $^3J_{H3'-P}$ with percent of N conformer.[42] Second, RNA single strands display a different behavior with respect to temperature compared to DNA single-strands. When the temperature was lowered (i.e., the population of stacked conformers was increased), $^3J_{H3'-P}$ of RNA oligomers increased from ca. 8 to >9 Hz, whereas in DNA oligomers, a decrease was observed from 6–7 to <5 Hz.[43] Third, a ^{1}H and ^{31}P NMR study of ApA and dApdA indicated that both phosphate groups are predominantly in the ϵ^t state.[59] However, at high temperatures, the ϵ^- conformation becomes evident.[43] These results suggest the following:[43] (1) the torsion angle of ϵ^t is smaller in stacked RNAs than it is in DNAs (the same relationship is generally true for any N-type sugar compared to an S-type sugar); (2) the phosphate group prefers to occupy the ϵ^t range in the stacked state. $^3J_{H3'-P}$ values for the DNA duplex, d(CGCGAATTCGCG)$_2$, are smaller (2.8–6.3 Hz) than those previously found for single strands.[28] This finding is consistent with the correlation mentioned above of decreased coupling with increased stacking.

For *cis*-Pt$(NH_3)_2${d(TCTCGGTCTC)-N7(5),N7(6)}, six $^3J_{H3'-P}$ (6.1–7.1 Hz and ϵ^t values of 201–206°) are in the range typically observed for single-strand DNA (Table I). *Four of these are located in the region 3′ to the Pt binding site.* ^{1}H NMR analysis[16] indicates that the sugar of G_5 has an N-type conformation, which should result in a $^3J_{H3'-P}$ value of 8–10 Hz. In fact, a value of ~8.5 Hz is found. The remaining two H3′–P pairs with large coupling constants are C_2p (8.9 Hz) and T_3p (8.0 Hz), both with unusual ^{31}P chemical shifts. The observation of large $^3J_{H3'-P}$ values is most readily rationalized in terms of distortions of the normal angles from those found for single-stranded DNA. Even if the measured coupling constants reflect a conformational average, the results imply an increase in the C4′–C3′–O3′–P torsional angle in these regions. It is also noteworthy that the intensities of cross peaks observed in the SRCSC and 2D *J* experiments for G_5p, C_2p, and T_3p are weaker than those observed for the H3′–P pairs with smaller coupling constants (Figure 11). Two reasons for this effect may be suggested. First, if the H3′ signal is broad, a shorter relaxation time is indicated and the intensity of the 2D cross peak would be decreased. G_5 H3′ is significantly broader than other resolved H3′ signals for this oligomer. The line width of C_2 and T_3 H3′ signals may be broad but cannot be directly observed due to overlap with several other H3′ signals. Second, depending on the magnitude of coupling with other protons, cancellation of antiphase components in COSY-type experiments such as SRCSC may occur. The G_5 sugar exists in an N-type conformation rather than the S type typically observed for DNA, resulting in different coupling constants for H3′ with H2′/H2″ and H4′. The sugars of C_2 and T_3 may also exist in nontypical conformations because of the distorted structure in this region.

In the ^{1}H NMR spectrum of *cis*-Pt$(NH_3)_2${d(TCTCGGTCTC)-N7(5),N7(6)} at 25 °C, the G_6 H8 signal at 9.37 ppm is broad.[15] As the temperature was increased, this signal steadily shifted upfield to 9.07 ppm and sharpened (Figure 7). The linear nature of this shift is consistent with the ^{31}P NMR and UV results (see above). At 70 °C, the signals of G_5 H8 (8.10 ppm) and G_6 H8 (9.10 ppm) are sharp, with chemical shift values very similar to those reported for *cis*-Pt$(NH_3)_2${d(TGGT)-N7-(2),N7(3)}.[11] In this oligomer, the fairly sharp 5′ and 3′ G H8 signals occurred at 9.04 and 8.25 ppm, respectively. This similarity suggests a close resemblance of the Pt binding site structure of *cis*-Pt$(NH_3)_2${d(TCTCGGTCTC)-N7(5),N7(6)} at high temperature to that of the short single-strand *cis*-Pt$(NH_3)_2${d-(TGGT)-N7(2),N7(3)}. However, at lower temperatures, G_6 H8 is less shielded and G_5 H8 is more shielded, consistent with a distorted structure such as model I.

The ^{1}H NMR spectra of the Pt(en) and *cis*-Pt$(MeNH_2)_2$ adducts at 25 °C each exhibit a broad downfield signal assigned to G_6 H8 by analogy with *cis*-Pt$(NH_3)_2${d(TCTCGGTCTC)-N7-(5),N7(6)} assignments. However, for both adducts, this signal is ~0.3 ppm upfield of the *cis*-Pt$(NH_3)_2$ adduct G_6 H8, indicating greater shielding. The G_5 H8 signal of *cis*-Pt$(MeNH_2)_2${d-(TCTCGGTCTC)-N7(5),N7(6)} is fairly sharp and is 0.15 upfield of G_5 H8 for the *cis*-Pt$(NH_3)_2$ and Pt(en) adducts. The sharpness of the G_5 H8 signal and the broadness of two unusual ^{31}P NMR signals for *cis*-Pt$(MeNH_2)_2${d(TCTCGGTCTC)-N7(5),N7(6)} compared with the other two adducts indicates a greater flexibility in this chain. These effects of the amine ligand upon the G_5 and G_6 H8 signals provide further evidence for model I. At 70 °C, the G_6 H8 shift value for *cis*-Pt$(MeNH_2)_2${d-(TCTCGGTCTC)-N7(5),N7(6)} is similar to that reported for the 3′ G H8 of *cis*-Pt$(MeNH_2)_2${d(TGGT)-N7(5),N7(6)}, suggesting, like the *cis*-Pt$(NH_3)_2$ adduct discussed above, similarity of structure to that of the short single-strand at high temperature. The Pt(en) and *cis*-Pt$(MeNH_2)_2$ adducts each exhibit a methyl signal at 1.97 ppm, analogous to the T_7 Me signal observed with the *cis*-Pt$(NH_3)_2$ adduct. This chemical shift is unusually far downfield, and its similarity among the three adducts indicates

(42) Lankhorst, P. P.; Haasnoot, C. A. G.; Erkelens, C.; Altona, C. *J. Biomol. Struct. Dyn.* **1984**, *1*, 1387.
(43) Altona, C. *Recueil* **1982**, *101*, 413.
(44) Sundaralingam, M. *Biopolymers* **1968**, *6*, 189.
(45) Sundaralingam, M. *Biopolymers* **1969**, *7*, 821.
(46) Pullman, B.; Perahiia, D.; Saran, A. *Biochim. Biophys. Acta* **1972**, *269*, 1.
(47) Altona, C. In *Structure and Conformation of Nucleic Acids and Protein-Nucleic Acid Interaction*; Sundaralingam, M., Rao, S. T., Eds.; University Park Press: Baltimore, 1975; p 613.
(48) Altona, C.; van Boom, J. H.; de Jager, J. R.; Koeners, H. J.; van Binst, G. *Nature (London)* **1974**, *247*, 558.
(49) Davies, D. B.; Sadikot, H. *Biopolymers* **1983**, *22*, 1843.
(50) Yokoyama, S.; Inagaki, F.; Miyazawa, T. *Biochemistry* **1981**, *20*, 2981.
(51) Blonski, W. J. P.; Hruska, F. E.; Sadana, K. L.; Loewen, P. C. *Biopolymers* **1983**, *22*, 605.
(52) Jack, A.; Ladner, J. E.; Klug, A. J. *J. Mol. Biol.* **1976**, *108*, 619.
(53) Ezra, F. S.; Lee, C.-H.; Kondo, N. S.; Danyluk, S. S.; Sarma, R. H. *Biochemistry* **1977**, *16*, 1977.
(54) Niemczura, W. P.; Hruska, F. E. *Can. J. Chem.* **1980**, *58*, 472.
(55) Dhingra, M. M.; Saran, A. *Biopolymers* **1982**, *21*, 859.
(56) Altona, C.; van Boom, J. H.; Haasnoot, C. A. G. *Eur. J. Biochem.* **1976**, *71*, 557.
(57) Wood, D. J.; Ogilvie, K. K.; Hruska, F. E. *Can. J. Chem.* **1975**, *53*, 2781.
(58) Evans, F. E.; Lee, C.-H.; Sarma, R. H. *Biochem. Biophys. Res. Commun.* **1975**, *63*, 106.
(59) Lee, C.-H.; Evans, F. E.; Sarma, R. H. *FEBS Lett.* **1975**, *51*, 73.

that the structure of the oligomer at this site (T_7) is the same.

As mentioned above, *cis*-Pt(NH_3)$_2${d(TCTCGGTCTC)-N7(5),N7(6)} is well characterized. Since several types of experiments were not repeated previously with this platinated oligomer, we performed additional types of experiments, some of which (electrophoresis, ^{17}O labeling, UV melting, SRCSC, 2D *J*) were discussed above. Furthermore we carried out two studies that would provide some additional basis for future investigations of more complex systems. First, ^{195}Pt NMR spectroscopy of *cis*-Pt(NH_3)$_2${d(TCTCGGTCTC)-N7(5),N7(6)} reveals a single signal at −2450 ppm; this chemical shift is very similar to values reported for *cis*-Pt(NH_3)$_2$(GMP)$_2$ (−2455 ppm) and *cis*-Pt(NH_3)$_2$(Guo)$_2$ (−2445 ppm).[34] In both of these compounds, the Pt is bound to two guanine residues via N7. These results suggest that no unusual distortion has occurred at the Pt moiety itself, since Pt chemical shifts are very sensitive to changes in the ligand or in N–Pt–N bond angles.[34,35] Second, studies of the ^1H aromatic region upon addition of $Cu(NO_3)_2$ to a *cis*-Pt(NH_3)$_2${d(TCTCGGTCTC)-N7(5),N7(6)} solution indicate Pt binding at the N7 of both G moieties. Relatively little broadening of G_5 and G_6 H8 signals was observed. H8 signals of platinated poly(I)–poly(C) residues have also been observed even at high concentrations of Cu^{2+}.[33] den Hartog et al.[17] employed pH titration to establish N7 coordination, but this method is not applicable to all cases because of precipitation or aggregation. Thus, the absence of line broadening of H8 signals on addition of Cu^{2+} appears to be a useful alternative to pH titration as a means of assessing Pt coordination at N7 of 6-oxopurines.

After duplexation with the complementary strand d(GAGACCGAGA), the ^{31}P NMR spectrum of *cis*-Pt(NH_3)$_2${d(TCTCGGTCTC)-N7(5),N7(6)} exhibits two signals with unusual chemical shifts.[7] The downfield signal at −3.2 ppm and the upfield signal at −4.9 ppm have been assigned as G_5pG_6 and C_4pG_5, respectively.[7] A SRCSC experiment conducted with [*cis*-Pt(NH_3)$_2${d(TCTCGGTCTC)-N7(5),N7(6)}]–d(GAGACCGAGA) at 22 °C (Figure 12) gave $^3J_{HCOP}$ values for G_5p and C_4p that are very similar to those measured for the same moieties in the single strand. In addition, in both cases these signals have low intensities. The chemical shifts of the G_5 and C_4 H3′ signals are also very similar in the single strand and the duplex. These results and the similar shifts of the $C_4pG_5pG_6$ ^{31}P signals indicate that the structure of the region $C_4G_5G_5$ does not change significantly upon duplexation. In most cases, duplexes containing a *cis*-PtA_2{d(GG)-N7,N7} moiety exhibit only one unusual ^{31}P signal.[60,61] Obviously, for *cis*-Pt(NH_3)$_2${d(TCTCGGTCTC)-N7(5),N7(6)}, some unusual interaction, e.g., a hydrogen bond between the C_4pG_5 phosphate and an amine ligand or CG stacking, stabilizes the CGG structure.

Temperature variation studies were conducted on the [*cis*-Pt(NH_3)$_2${d(TCTCGGTCTC)-N7(5),N7(6)}]–d(GAGACCGAGA) duplex. The ^{31}P NMR spectrum of the platinated duplex underwent some interesting transformations with increasing temperature.[7] At 13 °C, only two unusually shifted ^{31}P signals are present: G_5pG_6 at −3.3 ppm and C_4pG_5 at −5.0 ppm. Both signals are slightly broadened compared to analogous signals in the single strand. In comparing ^{31}P NMR spectra of the platinated single strand and duplex, it is also of interest that while the C_4pG_5 signal is shifted further away from the normal range (in the upfield direction) in the duplex than in the single strand, the duplex G_5pG_6 signal is shifted closer to the normal range (in the upfield direction). Evidently, the C_4pG_5 phosphate becomes more distorted, and the G_5pG_6 phosphate becomes more normal upon duplexation. Of course, all other signals are in the normal range in the duplex.

Upon increase of temperature, both signals (C_4pG_5 and G_5pG_6) exhibited sigmoidal shifts in the downfield direction. Between 13 and 30 °C, the signals broadened severely. Upon further temperature increase, the signals sharpened. The T_m of this transition is ∼32 °C. The sigmoidal shifting of the unusually shifted signals correspond to the sharp transition in the UV melt.

Scheme I. Representation of Distorted Duplex and Effects of Increasing Temperature (to the Right)

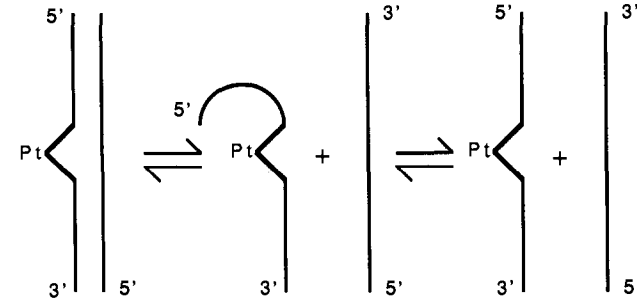

The T_m of duplex disruption depends upon concentration.[36,62,63] The concentration of the NMR sample was ∼30 times that of the UV sample, accounting for the 6 °C higher T_m for the NMR experiment.

Between 45 and 65 °C, a signal shifted downfield out of the normal range and then back. This signal is probably the downfield signal assigned as C_2pT_3 in the single strand. In this temperature range, a second broad transition, probably due to the melting of the looped-back structure of the platinated single strand, was observed in the UV melt.

The temperature dependence of the ^1H NMR spectrum of [*cis*-Pt(NH_3)$_2${d(TCTCGGTCTC)-N7(5),N7(6)}]–d(GAGACCGAGA) was also examined (Figure 10). As the temperature was increased from 20 to 40 °C, the downfield G_5 H8 signal[16] broadened and then disappeared. There was no change in chemical shift in this temperature range. The G_6 H8 signal[16] is in a crowded region and was not monitored. This line broadening is caused by the melting of the duplex form and corresponds to the sharp sigmoidal transition observed with UV and ^{31}P NMR methods. At ∼55 °C, a broad signal appeared at 9.0 ppm. This chemical shift value is similar to that of G_6 H8 of *cis*-Pt(NH_3)$_2${d(TCTCGGTCTC)-N7(5),N7(6)} at this temperature. At 70 °C, this signal sharpened and moved slightly downfield.

The temperature dependence of UV absorbance, ^{31}P NMR, and ^1H NMR indicates that [*cis*-Pt(NH_3)$_2${d(TCTCGGTCTC)-N7(5),N7(6)}]–d(GAGACCGAGA) undergoes two structural transitions, as shown in Scheme I.

At 25 °C, the oligomer is in the duplex form. As the temperature increased, the duplex melted. This transition is characterized by sigmoidal changes in UV absorbance and in the positions of the unusually shifted ^{31}P signals, and by G H8 chemical shift changes. As the duplex is melted, the *cis*-Pt(NH_3)$_2${d(TCTCGGTCTC)-N7(5),N7(6)} looped-back structure (model I) is formed. This is indicated by the appearance of ^{31}P and ^1H signals characteristic of this structure. As the temperature is increased further, the looped-back structure is disrupted. This occurrence is characterized by the higher temperature broad transition in the UV melt, the shift of the C_2pT_3 signal into the normal range in the ^{31}P NMR spectrum, and the appearance at 9.0 ppm and sharpening of the G_6 H8 signal in the ^1H NMR spectrum.

Summary. We have confirmed many of the previous findings reported by the Reedijk group and have results totally consistent with their findings.[7,16,17] In addition to placing some of these findings on a firmer basis, the 2D ^{31}P NMR spectroscopy and the ^{17}O-labeling studies provide further insight into the nature of the distorted single-strand structure. For the platinated adducts, the similar $^3J_{HCOP}$ values for G_5p and C_4p strongly suggest that the $C_4G_5G_6$ trinucleotide region has a similar structure in both the single-strand and duplex species. This trinucleotide unit may play some role in favoring the looped-back model I structure we have proposed. It remains to be seen whether other platinated oligonucleotides, with different sequences, possess these unusual spectral and structural features.

(60) Caradonna, J. P.; Lippard, S. J. *Inorg. Chem.* **1988**, *27*, 1454.
(61) Unpublished results from this lab.
(62) Manning, G. S. *Q. Rev. Biophys.* **1978**, *11*, 179.
(63) Record, M. T.; Anderson, C. F.; Hohman, T. M. *Q. Rev. Biophys.* **1978**, *11*, 103.

Acknowledgment. This work was supported by NIH Grant GM 29222 to L.G.M. and by NSF Grant DMB8604304 to D.L. NMR instrumentation was supported by grants from NIH and NSF. We thank Dr. Robert Jones (Emory) for his assistance with the GN-500 spectrometer and Drs. Dan Bancroft and Steve Hollis for helpful discussions.

Registry No. d(TCTCGGTCTC), 88904-80-7; d(GAGACCGAGA), 88904-81-8; d(TCTCGGTCTC)-d(GAGACCGAGA), 88904-82-9; *cis*-$Pt(NH_3)_2Cl_2$, 15663-27-1; $Pt(en)Cl_2$, 14096-51-6; *cis*-$Pt(MeNH_2)_2Cl_2$, 15273-32-2; *cis*-$Pt(NH_3)_2$[d(TCTCGGTCTC)-N7(5),N7(6)], 98478-95-6; Pt(en)[d(TCTCGGTCTC)-N7(5),N7(6)], 121808-76-2; *cis*-$Pt(MeNH_2)_2$[d(TCTCGGTCTC)-N7(5),N7(6)], 121808-77-3; *cis*-$Pt(NH_3)_2$[d(TCTCGGTCTC)-N7(5),N7(6)]-d(GAGACCGAGA), 110975-19-4.

Supplementary Material Available: Tables of temperature dependence of ^{31}P NMR signals and UV melting data and a contour plot of a ^1H-detected ^1H-^{31}P 2D J correlation map of *cis*-$Pt(NH_3)_2$[d(TCTCGGTCTC)-N7(5),N7(6)] (4 pages). Ordering information is given on any current masthead page.

Novel Diastereomers with Opposite Chirality at Ruthenium Formed by N7,α-PO_4 Chelation of 5'-dGMP to the Antimetastatic Agent *trans*-$RuCl_2(DMSO)_4$: NMR and CD Evidence

Enzo Alessio,*,† Yinghai Xu,‡ Sabina Cauci,§ Giovanni Mestroni,† Franco Quadrifoglio,§ P. Viglino,§ and Luigi G. Marzilli*,‡,⊥

Contribution from the Department of Chemical Sciences, University of Trieste, 34127 Trieste, Italy, Department of Chemistry, Emory University, Atlanta, Georgia 30322, and Institute of Biology, University of Udine, 33100 Udine, Italy. *Received December 14, 1988*

Abstract: A novel diastereomeric pair of isomers was discovered in an initial study of the interaction of the antimetastatic agent *trans*-$RuCl_2(DMSO)_4$ with nucleic acid components. In particular, 5'-dGMP forms two products that have characteristic features clearly indicating that the guanine N7 and the α-phosphate group form a chelate to the metal center. These features include (a) a pronounced downfield shift of the ^{31}P NMR signals of the chelates; (b) a downfield shift of the H8 ^1H NMR signals of the guanine in the chelates—this downfield shift persists in monodentate N7 coordinated forms favored by protonation of the phosphate group at acid pH; and (c) characteristic changes in the shifts and coupling constants of the deoxyribose ^1H NMR signals. This unusual chelation mode of binding has been characterized by NMR spectroscopy in only two previous studies. Interestingly, these studies involved other classes of metalloanticancer agents, namely Pt(II) and metallocene drugs. However, in these latter classes of drugs, only one isomer was possible. In the Ru derivatives studied here, the octahedral configuration leads to the possibility of diastereomers. After separation of the chelates by HPLC, the isomers were found to have nearly identical UV absorption spectra and a weak visible band at ~410 nm. However, the CD spectra have bands that have opposite signs but similar intensities and positions. Thus, the compounds are isomers that differ principally by having an opposite chirality at ruthenium. Analysis of several types of experiments demonstrated that the isomers have the composition $[Ru^{II}Cl(H_2O)(DMSO)_2(5'\text{-dGMP})]^-$. In contrast to the widely studied Pt(II) anticancer agents, the Ru drug does not readily bind to two 5'-dGMP at neutral pH. Thus, in addition to stereochemical differences between the octahedral Ru(II) and square-planar Pt(II) drugs, the Ru(II) compounds may not easily form the N7,N7 GpG crosslink characteristic of the DNA adducts formed by Pt anticancer drugs. Should the Ru(II) drugs form such a crosslink form, however, two diastereomers, with opposite chirality at Ru, are possible.

Two important recent topics in metal–nucleic acid and metal–nucleotide chemistry have been the following: (a) the elucidation of the mechanism of action of metalloantineoplastic agents[1] and (b) the exploitation of metal complex chirality in exploring nucleic acid structure and biochemistry.[2] Although chiral metal anticancer drugs could bind more selectively to DNA, the likely cellular target, only modest success has been achieved thus far in such endeavors.[3] Most chiral anticancer agents studied have been pseudosquare-planar platinum compounds.[1,3] Since the chirality is centered on the nonleaving ligand, the effects of chirality are expected to be less important in square-planar complexes than in pseudooctahedral complexes,[2] where the chirality is centered on the metal.

The great success of the drug *cis*-$PtCl_2(NH_3)_2$ (cisplatin) has encouraged the search for anticancer agents with other transition metals.[4] We have shown that *cis*- and *trans*-$Ru^{II}Cl_2(DMSO)_4$ have good antimetastatic activity against several murine metastasizing tumors.[5,6] Moreover, the complexes were found to possess

† University of Trieste.
‡ Emory University.
§ University of Udine.
⊥ L.G.M. is also a member of the Winship Cancer Center.

(1) Fitchtinger-Schepman, A. M. J.; Van der Veer, J. L.; den Hartog, J. H. J.; Lohman, P. H. M.; Reedijk, J. *Biochemistry* **1985**, *24*, 707. Sherman, S. E.; Lippard, S. J. *Chem. Rev.* **1987**, *87*, 1153. Lippard, S. J. *Pure Appl. Chem.* **1987**, *59*, 731. Reedijk, J. *Pure Appl. Chem.* **1987**, *59*, 181 and references therein.

(2) Barton, J. K.; Lolis, E. *J. Am. Chem. Soc.* **1985**, *107*, 708. Barton, J. K.; Danishefsky, A. T.; Goldberg, J. M. *J. Am. Chem. Soc.* **1984**, *106*, 2172. Barton, J. K.; Basile, L. A.; Danishefsky, A. T.; Alexandrescu, A. *Proc. Natl. Acad. Sci. U.S.A.* **1984**, *81*, 1961. Barton, J. K.; Raphael, A. L. *J. Am. Chem. Soc.* **1984**, *106*, 2466.

(3) Kidani, Y. In *Platinum and Other Metal Coordination Compounds in Cancer Chemotherapy*; Nicolini, M., Ed.; Martinus Nijhoff: Boston, MA, 1988; p 555.

(4) Clarke, M. J. In *Metal Ions in Biological Systems*; Siegel, H., Ed.; Marcel Dekker: New York/Basle, 1980; Vol. 11, p 231. Clarke, M. J.; Galang, R. D.; Rodriguez, V. M.; Kumar, R.; Pell, S.; Bryan, D. M. In *Platinum and Other Metal Coordination Compounds in Cancer Chemotherapy*; Nicolini, M., Ed.; Martinus Nijhoff: Boston, MA, 1988; p 582. Keppler, B. K.; Wehe, D.; Endres, H.; Rupp, W. *Inorg. Chem.* **1987**, *26*, 844. Keppler, B. K.; Schmael, D. *Arzeim.-Forsch.* **1986**, *36*, 1822. Köpf-Maier, P.; Köpf, H. *Chem. Rev.* **1987**, *87*, 1137.

0002-7863/89/1511-7068$01.50/0